Aus dem Zentrum für Therapieforschung - Institut für Pharmakologie

der Medizinischen Fakultät Charité – Universitätsmedizin Berlin

DISSERTATION

Modulatory effects of Cav1.3 calcium channels on dopamine homeostasis and alpha synuclein expression in a mouse model of Parkinson's disease

Die modulatorische Rolle von Calciumkanälen vom Subtyp Cav1.3 auf die Dopaminhomöostase und die Alpha-Synuclein-Expression in einem Mausmodell für den Morbus Parkinson

zur Erlangung des akademischen Grades
Doctor medicinae (Dr. med.)

vorgelegt der Medizinischen Fakultät
Charité - Universitätsmedizin Berlin

von

Qingzhou Fei
aus Shanghai, China

Datum der Promotion: 30. Juni 2024

Table of Contents

List of figures

List of tables

1 List of Abbreviations

6-OHDA	6-Hydroxydopamine
AADC	L-aromatic amino acid decarboxylase
ABI	Applied Biosystems
aSYN	alpha synuclein
ATP	adenosine triphosphate
ATP13A2	ATPase 13A2
BBB	blood brain barrier
BG	basal ganglia
BSA	bovine serum albumin
CCAs	calcium channel antagonists
cDNA	complementary DNA
COMT	catechol-O-methyl transferase
CPu	caudate putamen
CSF	cerebrospinal fluid
Ct	cycle threshold
DA	dopamine
DAT	dopamine transporters
DBS	deep brain stimulation
DHP	dihydropyridines
DJ-1	protein deglycase DJ-1
DNA	deoxyribonucleic acid
DOPAC	3,4-Dihydroxyphenylacetic acid
DTT	1,4-dithio-DL-threitol
EDTA	ethylenediaminetetraacetic acid
ER	endoplasmic reticulum
GABA	gamma aminobutyric acid
GP	globus pallidus
GPe	globus pallidus external
GPi	globus pallidus internal
GWAS	genome-wide association studies
IPD	idiopathic Parkinson’s disease
KO	knockout
LB	Lewy bodies

L-DOPA	L-3,4-dihydroxyphenylalanine
LRRK-2	leucine rich repeat kinase 2
MAO	monoamine oxidase
MOA-B	monoamine oxidase-B
MPTP	1-Methyl-4-phenyl-1,2,3,6-tetrahydropyridine
mRNA	messenger RNA
NF-κB	nuclear factor kappa B
OXPHOS	oxidative phosphorylation
PARK1	α-synuclein gene
PARK2	E3 ubiquitin-protein ligase parkin
PARK6	PTEN-induced putative kinase 1, PINK1
PARK7	protein deglycase DJ-1, DJ-1
PARK8	leucine rich repeat kinase 2, LRRK-2
PBS	phosphate buffered saline
PD	Parkinson's disease
PINK1	PTEN-induced putative kinase 1
PVDF	polyvinylidene fluoride
qPCR	quantitative real-time PCR
RNA	ribonucleic acid
ROS	reactive oxygen species
RT	room temperature
SDS	sodium dodecyl sulfate
SN	substantia nigra
SNc	substantia nigra pars compacta
SNr	substantia nigra reticularis
SNCA	alpha-synuclein gene
STN	subthalamic nucleus
TAE	Tris base, acetic acid & EDTA
TBS	Tris-buffered saline
TEMED	Tetramethylethylenediamine
TH	tyrosine hydroxylase
VTA	ventral tegmental area
WB	Western blot

2 Abstract

2.1 Summary

In Parkinson's disease (PD), mitochondrial dysfunction has been suggested to be an important pathogenetic factor whereby calcium and α-synuclein (aSYN) pathology facilitate the selective death of substantia nigra neurons.

The present study aimed at investigating the modulatory effects of the voltage-gated calcium channels of subtype 1.3 ($Ca_v1.3$) on dopamine (DA) homeostasis and aSYN expression in $Ca_v1.3$ channel knockout mice under mitochondrial dysfunction induced by the neurotoxin 1-methyl-4-phenyl-1,2,3,6-tetrahydropyridine (MPTP).

Following chronic MPTP treatment, tissue samples from the striatum and the midbrain were used for HPLC-based analysis of striatal DA and its metabolites, for the assessment of nigral mRNA levels of tyrosine hydroxylase (TH), dopamine transporter (DAT), and aSYN, as well as for Western blot detection of TH, DAT and aSYN protein in the striatum and the midbrain.

$Ca_v1.3$ channel knockout mice displayed a decreased vulnerability to chronic MPTP exposure as measured by a rescue of striatal DA of ~50% and an unaffected DA turnover. This neuroprotective effect was paralleled by a preserved mRNA expression of nigral TH and DAT. However, such an effect could not be observed for the protein expression of striatal DAT nor for striatal and nigral aSYN protein when compared to MPTP-treated wild-type mice.

Our data underline the pivotal role of $Ca_v1.3$ channels in the propagation of MPTP-induced breakdown of the nigro-striatal DA system. However, we could not confirm in-vivo evidence that aSYN expression is linked to calcium overload under the condition of mitochondrial dysfunction. For the first time we could demonstrate that genetic "silencing" of $Ca_v1.3$ channels in mice mitigates the toxic actions of chronic MPTP exposure, which so far has only been shown pharmacologically using non-selective calcium-channel blockers.

2.2 Zusammenfassung

Bei der Pathophysiologie des Idiopathischen Parkinson-Syndroms stellt die mitochondriale Dysfunktion einen wichtigen pathogenetischen Faktor dar, bei dem Calcium und Alpha-Synuclein den selektiven Untergang von Neuronen der Substantia nigra fördern.

Die vorliegende Studie zielte darauf ab, die modulatorische Rolle von spannungsgesteuerten Calciumkanälen vom Subtyp $Ca_v1.3$ auf die Dopaminhomöostase und die Alpha-Synuclein-Expression in $Ca_v1.3$-knockout Mäusen unter der Bedingung einer mitochondrialen Dysfunktion, die durch das Neurotoxin 1-Methyl-4-phenyl-1,2,3,6-tetrahydropyridin (MPTP) induziert wurde, zu untersuchen.

Dazu wurden im Anschluss an eine chronische MPTP-Behandlung Gewebeproben von Striatum und Mittelhirn sowohl für die HPLC-basierte Analyse des striatalen Gehaltes von Dopamin und seinen Metaboliten, als auch für die Bestimmung der nigralen mRNA Level von Tyrosinhydroxylase (TH), Dopamintransporter (DAT) und Alpha-Synuclein (A-Syn) sowie für die Westernblot Detektion von TH-, DAT- und A-SYN-Protein im Striatum und im Mittelhirn untersucht.

Im Ergebnis zeigte sich bei den $Ca_v1.3$-knockout Mäusen eine geringere Vulnerabilität auf die chronische MPTP-Exposition gemessen an einer Erhaltung des striatalen Dopamingehaltes von 50% und einem unveränderten Dopaminumsatz. Dieser neuroprotektive Effekt war begleitet von einer intakten mRNA-Expression von TH und DAT in der Substantia nigra. Allerdings konnte im Vergleich zu MPTP-behandelten Wildtyp-Mäusen ein derartiger Effekt weder für die Protein-Expression des striatalen DAT, noch für das striatale und nigrale A-Syn-Protein beobachtet werden.

Unsere Daten unterstreichen die zentrale Rolle von $Ca_v1.3$-Kanälen bei der Propagation der MPTP-induzierten Schädigung des nigro-striatalen Dopamin-Systems. Dennoch fanden wir keine in-vivo Evidenz für eine an die Calcium-Überladung gekoppelte A-Syn-Expression unter mitochondrialer Dysfunktion. Zum ersten Mal konnten wir demonstrieren, dass eine genetische Suppression von $Ca_v1.3$-Kanälen in Mäusen die toxischen Effekte einer chronischen MPTP-Exposition abmildern kann, was bisher nur pharmakologisch, d.h. unter Verwendung nicht-selektiver Calciumkanalblocker gezeigt wurde.

3 Introduction

3.1 Parkinson's Disease-definition and epidemiology

Parkinson's disease is a clinically and pathologically defined progressive multisystem disorder affecting distinct areas of the central and even peripheral nervous system.

Historical background:

In his monograph "An essay on the shaking palsy" published in 1817, *James Parkinson* described several patients who were clinically characterized by the presence of resting tremor, gait disorder and bradykinesia (Parkinson, 2002). Later on, *Charcot* described rigidity as a further clinical symptom and suggested to refer the symptomatic triad as Parkinsonian syndrome or parkinsonism (Lees, 2007).

Clinical parkinsonism vs. Parkinson's disease:

According to current terminology, Parkinsonian syndrome describes a bradykinesia-rigidity movement disorder in which bradykinesia is the obligate and leading symptom along with at least one of the additional signs like resting tremor, rigidity or postural instability. Thus, parkinsonism must be differentiated from Parkinson's disease (PD) which is regarded as an own entity in a group of neurodegenerative disorders. Clinically, patients with PD exhibit in addition to motor symptoms also non-motor symptoms like hyposmia, constipation, orthostatic dysregulation, depression and cognitive impairment.

Epidemiology:

PD is the second most common neurodegenerative disease, affecting 2 to 3% of the population > 65 years of age (de Lau and Breteler, 2006). The overall incidence in industrialized countries is 0.3% with a lifetime risk of 2% (Nussbaum and Ellis, 2003). In an article of systematic review and meta-analysis, the authors estimated the overall prevalence of PD among those aged ≥45 years to be 572 per 100,000 in North America (Marras et al., 2018). Several studies also found that the prevalence of PD increased with age, was higher in men than in women, and varied by geographic location (Poewe et al., 2017).

3.2 Basic pathophysiology of Parkinson's disease

Despite clinically phenotypic heterogeneity, the pathological hallmark of PD is characterized by the loss of dopamine containing neurons in the substantia nigra pars compacta (SNc) in the presence of intracellular inclusions containing aggregates of alpha-synuclein (Poewe et al.,

2017). The cardinal motor manifestations of PD patients are attributable to striatal dopamine deficiency resulting from the progressive dopamine neuron loss (see Figure 3-1). However, neurodegeneration also occurs in other brain neurotransmitter systems (e.g. cholinergic, adrenergic, serotoninergic) and is thought (at least in part) to be responsible for non-motor symptoms of PD (Surmeier et al., 2017a).

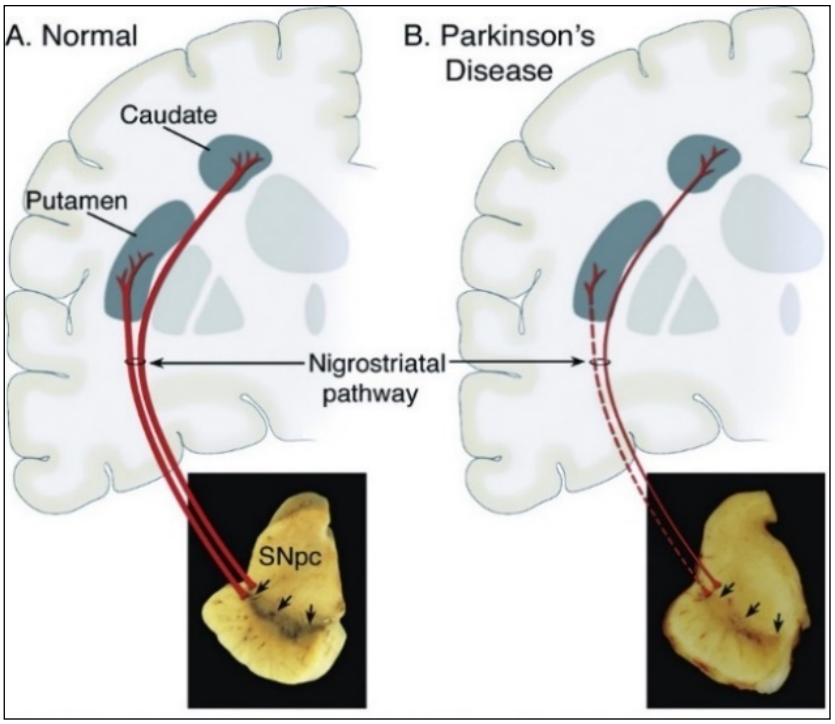

Figure 3-1 Neuropathology of Parkinson's Disease

The cell bodies of dopaminergic neurons are located in the SNc and project (red line) to the striatum (i.e. putamen and caudate nucleus). Normal pigmentation of the SNc is shown in (A). In PD, the degeneration of DA-ergic midbrain neurons virtually results in a depigmentation of the SNc, indicating the marked neuron loss which in turn leads to a breakdown of the nigrostriatal pathway that projects to the caudate-putamen (dashed line). Note: Caudate and putamen are shown in a coronal brain section whereas SNc is shown in an axial brain section. Adapted from (Dauer and Przedborski, 2003)

As mentioned above, the neurodegenerative process in the SNc is associated with an accompanying formation of intracellular inclusion (first described by Lewy, they are referred to as Lewy bodies), which have been identified as the accumulation of alpha synuclein (aSYN). For this reason, PD can also be classified as an alpha synucleinopathy (Calabresi et al., 2023). Recently, further molecules have been identified (i.e. mitochondrial and other membrane lipids like ubiquitin (Ub), and phosphorylated Ub) that are associated with aSYN aggregates (George

et al., 2013; Rocha Cabrero and Morrison, 2022). In a substantia nigra proteomic study, 204 proteins were identified that display significant expression level changes in PD patients versus controls, implicating that the pathogenic processes include mitochondrial dysfunction, oxidative stress, and cytoskeleton impairment (Licker et al., 2014).

aSYN is a 140 amino acid protein, encoded by the *SNCA* gene (Venda et al., 2010). The physiological function of aSYN is still not fully understood, but it is known to be present in several parts of the neuron, including the presynaptic region. Current evidence suggests that aSYN may play a role in various cellular processes such as synaptic vesicle dynamics and intracellular trafficking. However, in terms of the pathogenesis of PD, aSYN is one of the major components of *Lewy* bodies (LBs) which have been identified as aggregated and misfolded forms of aSYN in the brains of PD patients (Ghiglieri et al., 2018). Regarding the conformational states of aSYN (the naïve protein is soluble), oligomers are thought to be toxic to neurons, and aSYN fibrils can spread both *in vitro* and *in vivo*, suggesting their critical role in the progression of PD. Recently, many studies and observational reports have supported this "prion-like" behavior of aSYN. For example, in mice, synthetic aSYN fibrils can spread to neighboring structures and can even create *Lewy* pathology in the SNc (Luk et al., 2012). Another study showed nigral *Lewy* body-enriched fractions containing pathological aSYN from postmortem PD brains can propagate while the soluble aSYN from the same nigral tissue cannot induce PD-like pathological process (Recasens et al., 2014). If aSYN aggregates in a small number of cells can lead to the spread of aSYN aggregates to multiple brain regions, then the therapies directed at aggregated aSYN could help to slow or even stop the spread. However, two monoclonal antibodies targeting aSYN, Prasinezumab and Cinpanemab did not show any neuroprotective effects in early-stage PD patients (Lang et al., 2022; Pagano et al., 2022), suggesting PD is not a "simple" disease.

The current understanding of PD suggests a "multiple hits" hypothesis, which proposes that the disease is caused by a combination of various factors (i.e. toxic stress, mitochondrial dysfunction, limited neuroprotective response) (Sulzer, 2007; Sulzer and Surmeier, 2013). In the following sections, pan-cellular risk factors (e.g., age and declining mitochondrial dysfunction, genetic mutations, environmental toxins, and inflammation) as well as cell-specific risk factors of PD (e.g., nigral DA system and calcium-based "pacemaking" mechanism of nigral neurons) will be elaborated upon.

3.2.1 Pan-cellular risk factors

Age is the single and most important risk factor for the development of sporadic PD (synonymous for idiopathic Parkinsonian syndrome, IPS), and disease incidence rises dramatically above the age of sixty (Nussbaum and Ellis, 2003). Although little is known about the basics of this phenomenon, it is speculated that disturbed neuronal mitochondrial metabolism is the key component (Boumezbeur et al., 2010). This may be due to the increase of mitochondrial DNA damage over lifetime, resulting in subsequent mitochondrial dysfunction and cell death. Specifically, for DA-ergic neuron death a gradual decline of 5-10 % per decade has been described even in healthy subjects (Naoi and Maruyama, 1999). Mitochondrial dysfunction in PD patients is related to a specific defect in the activity of respiratory chain complex I in the SNc, and it may be the most appropriate cause for neurodegeneration in PD by reducing the synthesis of ATP (Moon and Paek, 2015; Schapira et al., 1990) (see Figure 3-3).

Genetic factors and the identification of several gene mutations (serially numbered as *PARK1 to 13*) and encoding proteins by linkage analysis, positional cloning and genome-wide association studies confirmed the link to familial forms of PD. In brief, *PARK1* involves point mutations and multiplications in the aSYN gene *(SNCA)* (Polymeropoulos et al., 1997), whereupon the encoding protein (alpha synuclein) is the principal component of Lewy bodies. *PARK2* encodes the E3-ubiquitin-protein ligase Parkin and its loss-of-function mutation abolishes the neuroprotective properties of Parkin in DA-ergic neurons. For *PARK6* and *PARK7* recessive mutations have been identified in the genes encoding for PTEN-induced putative kinase 1 (*PINK1*) and protein deglycase DJ-1 *(DJ-1)* with respective loss-of-function mutations in early onset (<40 years) parkinsonism (Mouradian, 2002; Sulzer, 2007; Trinh and Farrer, 2013). *PARK8* involves mutations in the leucine-rich repeat kinase 2 (*LRRK-2*), a kinase encoding the protein Dardarin. The most common Gly2019Ser mutation in this gene has a worldwide frequency of 1% in sporadic cases (i.e. IPD) and 4% in patients with hereditary parkinsonism, making it as common as Multiple System Atrophy and Progressive Supranuclear Palsy (Lees et al., 2009). Moreover, large genome-wide association studies (GWAS) have identified several genetic loci that are associated with an increased risk of developing Parkinson's disease (Grenn et al., 2020).

Several studies have sought to define the pathogenetic role of environmental factors contributing to the aetiology of PD (Kamel et al., 2007; Tanner et al., 2009). Although environmental toxins like pesticides (e.g. rotenone) and heavy metals appear to increase the risk

of the development of PD, no specific agent has been clearly identified as causative (Cannon and Greenamyre, 2011).

In recent years, it has been suggested that inflammation-derived oxidative stress and cytokine-dependent toxicity may as well contribute to the degeneration of SNc neurons and accelerate the progression of the disease in human subjects with IPS. Activated microglia, accumulation of cytokines, nuclear factor kappa B (NF-κB) pathway activation, and oxidative damage to proteins in the cerebrospinal fluid (CSF) and brains of individuals with PD support the theory that the inflammatory processes may contribute to the progression of PD, which is also evident in post-mortem PD brains at autopsy and even in experimental models of PD (Tansey and Goldberg, 2010).

3.2.2 Cell-specific risk factors in PD

As mentioned before, PD may be regarded as a "multi-system disorder" affecting, in addition to DA-ergic neurons, a significant number of other central and peripheral neuronal populations that exhibit *Lewy* pathology and neurodegeneration (Sulzer and Surmeier, 2013). However, the core motor features are clearly linked to the degeneration and death of nigral dopamine neurons (i.e., SNc neurons). SNc neurons in turn constitute a tiny fraction of all the neurons in the brain (<0.0001%), which suggests that there must be cell-specific factors contributing to the aetiology of PD (Surmeier et al., 2010b).

3.2.3 Dopamine system and PD

The biosynthesis of DA derives from the aromatic amino acid tyrosine which is converted to L-3,4-dihydroxyphenylalanine (i.e., L-dopa) via the rate-limiting enzyme tyrosine hydroxylase (TH). Subsequently, L-dopa is converted to DA by decarboxylation in the presence of L-aromatic amino acid decarboxylase (AADC) (see Figure 3-2). After syntheses, DA is immediately sequestered to storage vesicles through an active transport process that requires vesicular monoamine transporter 2 (VMAT2) in preparation for the release of the transmitter after depolarization. After the release of the neurotransmitter into the synaptic cleft, the reuptake of DA is mediated by presynaptic dopamine transporters (DAT).

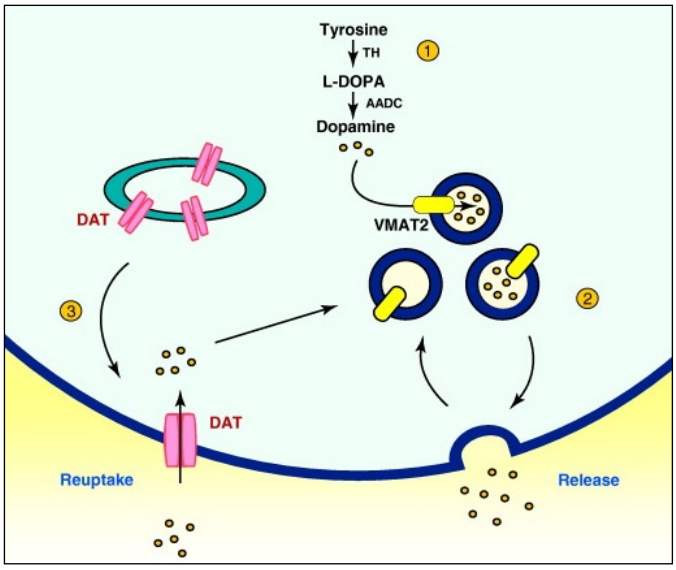

Figure 3-2 Dopamine synthesis, storage, release and reuptake

Dopamine is synthetized from L-dopa, which in turn requires tyrosine as a first educt and tyrosine hydroxylase (TH) as the rate-limiting enzyme. It is then stored in synaptic vesicles, which requires the active transport supported by vesicular monoamine transporter 2 (VMAT2), and released into the synaptic cleft, from where it can be reabsorbed by dopamine transporter (DAT). Adapted from Venda *et al.* (Venda et al., 2010)

After reuptake, DA is degraded by the enzymes catechol-O-methyl transferase (COMT) and monoamino oxidase (MAO) to 3,4-Dihydroxyphenylacetic acid (DOPAC), 3-methoxytyramine (3-MT) and homovanillic acid (HVA) as metabolites (Riederer et al., 1987). The compartmentalisation and metabolism of DA are crucial as cytosolic DA is prone to oxidation resulting in the formation of e.g. hydrogen peroxide and other reactive oxygen species (ROS), which in turn may trigger mitochondrial damage and cell death (Greenamyre and Hastings, 2004; Michel and Hefti, 1990; Zecca et al., 2003). Dysregulated DA storage and transport of DA can also contribute to increased oxidative stress and thus to elevated production of ROS and to cellular dysfunction (Uttara et al., 2009). Furthermore, there is a lot of *in vitro* evidence that DA and its auto-oxidative metabolites interact with aSYN by means of its polymerisation and aggregation (Leong et al., 2009). However, some other studies suggest DA itself is not the significant source for inducing cell death in PD. *Ulusoy* and colleagues found that elevated DA levels can increase the susceptibility to aSYN toxicity *in vivo*, but that DA is not the main factor determining aSYN-induced neurodegeneration in wild-type neurons (Ulusoy et al., 2012). Another study supports the notion that although L-dopa can be toxic to DA neurons *in vitro*, it is not likely to be toxic to DA neurons *in vivo*, and specifically in conditions such as PD (Mytilineou et al., 2003). Furthermore, VTA neurons, which also produce and release DA, are

not lost at the same rate in PD as SNc DA neurons are (Kish et al., 1988). Additionally, blocking DA synthesis does not show a neuroprotective effect to toxin-induced SNc neurodegeneration (Hasbani et al., 2005), and administration of L-DOPA or selective inhibitors of MAO-B in PD patients does not accelerate disease progression and have been even proposed to be neuroprotective (Fahn and Parkinson Study, 2005). Taken together, the different studies suggest that DA itself is likely not the key factor for triggering PD.

3.3 The role of calcium channels

3.3.1 Calcium channel and "pacemaking" nigral activity

Calcium (Ca^{2+}) acts as a second messenger of many signalling pathways that regulates the most fundamental and essential activities in neurons. In neurons, spiking activity refers to the generation and propagation of action potentials, which are electrical signals that spread through the axon of a neuron and cause the release of neurotransmitters at the synapse. When neurotransmitters bind to receptors on the postsynaptic neuron, it can trigger the opening of Ca^{2+} channels, resulting in an influx of Ca^{2+} ions into the cytosol and a subsequent increase in cytosolic Ca^{2+} levels. This increase in Ca^{2+} can trigger various downstream signaling pathways and modulate synaptic plasticity (Purves et al., 2018).

Voltage-gated calcium channels (VGCC) mediate controlled Ca^{2+} influx in response to membrane depolarization. The VGCCs are grouped into various subfamilies based on the pore-forming α1 subunit sequence homology as well as their functional and pharmacological properties: L-type VGCCs (Ca_v1 family), N-type VGCCs (Ca_v2 family), T-type VGCCs (Ca_v3 family), P/Q-type and R-type (Catterall et al., 2005).

The Ca_v1 family comprises four members of LTCC ($Ca_v1.1$–$Ca_v1.4$), which are known for their susceptibility to low nanomolar levels of dihydropyridines (DHP). They are called "L" channels because they produce long-lasting inward currents during depolarization. Among these members, $Ca_v1.2$ and $Ca_v1.3$ are found to be expressed in neurons and are primarily located in the somatodendritic regions (Zamponi et al., 2015).

3.3.2 The vulnerability of nigral dopamine (DA) neurons and the role of calcium channels

In the mammalian brain, the ventral part of the mesencephalon contains about 90% of the total number of DA-ergic neurons, with two overlapping nuclei that are rich in DA neurons in

midbrain: the SNc and the ventral tegmental area (VTA) (Chinta and Andersen, 2005). A low number (about 300 - 600 K in human and about 45 K in rat (Tansey and Goldberg, 2010)) of these neurons provide massive innervation into the striatum. Each SNc neuron might give rise to about 150,000 presynaptic terminals in the striatum, and SNc DA neurons also have massive dendrites that extend into the SNr (Oorschot, 1996). The SNc cell body represents far less than 1% of the total cell volume (Oorschot, 1996). However ventral midbrain dopamine neurons of the SNc preferentially degenerate in PD, while DA neurons in VTA near SNc are relatively not impaired. The molecular reason why the SNc neurons are much more vulnerable to PD triggers and to degeneration than the DA neurons in VTA are not fully understood (Surmeier et al., 2010a), and there are two main theories which may explain the selective vulnerability of nigral DA neurons.

The selective vulnerability of nigral DA neurons in the pathogenesis of PD has been attributed to a unique characteristic of these neurons. Unlike the vast majority of neurons of the brain, adult SNc neurons exhibit a continuous autonomous "pacemaking" activity of broad action potentials (2-4 Hz) irrespective of synaptic input (Surmeier et al., 2010b). $Ca_v1.2$ and $Ca_v1.3$ subunit contribute to this oscillation in SNc DA neurons. The $Ca_v1.3$ channels are particularly interesting because they open at relatively hyperpolarized membrane potentials (Surmeier et al., 2017b).

This "pacemaking" activity relies on Ca_v1-channels and this feature is different from most other neurons in the brain, even when compared with DA neurons of the VTA (Chan et al., 2010; Grace and Bunney, 1983). According to this molecular basis for "pacemaking", it was hypothesized that a permanent channel opening results in an increased calcium-related vulnerability of nigral DA neurons (Surmeier et al., 2010). More specifically, once the Ca^{2+} influx is complete, the use of Ca^{2+} ATPase pump and the Na^+/Ca^{2+} exchanger maintains the intracellular Ca^{2+} level: while extracellular Ca^{2+} is 1-2 mM, cytosolic Ca^{2+} is generally maintained at nanomolar levels (approximately 100 nM) (Zampese and Surmeier, 2020). The regulation of intracellular Ca^{2+} is a metabolically expensive process that requires the actions of ATPase pump, which results in increased mitochondrial activity and concomitant increased ROS generation (Surmeier et al., 2011). In most neurons, the Ca^{2+} influx is a rare process, and as a result it is easy to clear a small amount of Ca^{2+} that enters the cytoplasm. However, the situation in the SNc DA neurons is different because in SNc DA neurons the calcium channels open frequently and the events of Ca^{2+} influx occur at a comparatively high frequency (Wilson and Callaway, 2000).

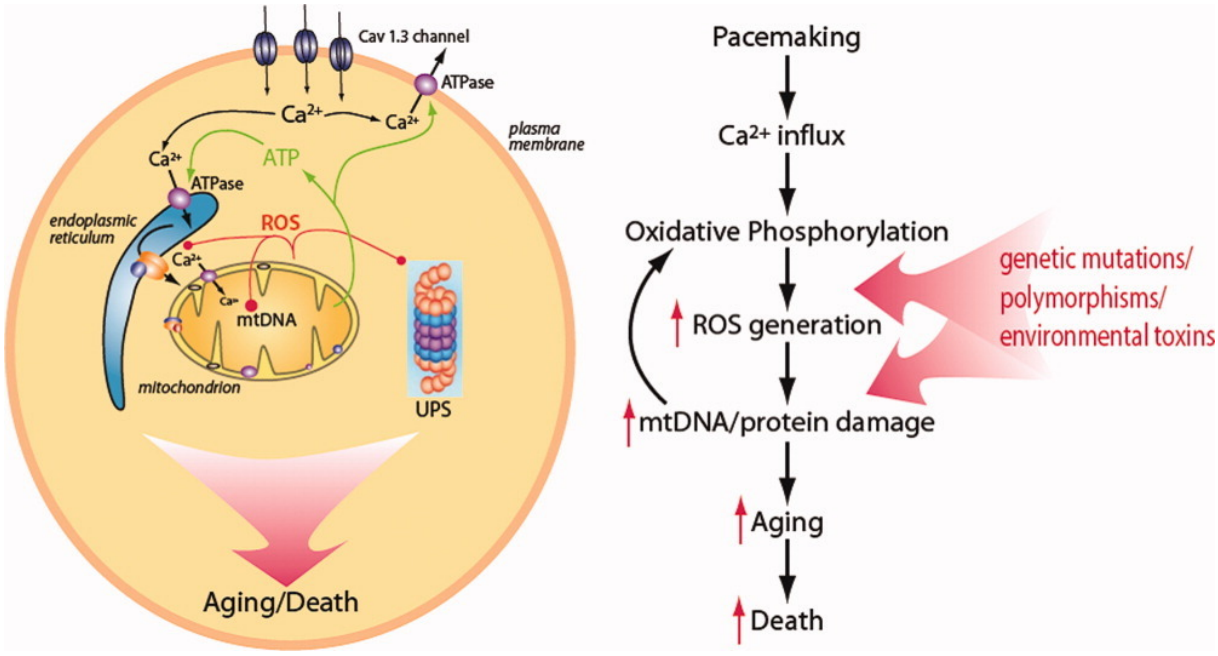

Figure 3-3 Schematic summarizing the key events in the aging model of PD

On the left, the figure shows a schematic of excessive Ca2+ influx during pacemaking in SNC DA neuron which can create a demand on oxidative phosphorylation and lead to oxidative stress through ROS production and cellular damage through mitochondrial dysfunction. On the right, the flow diagram shows genetic mutations or polymorphisms as well as environmental toxins could alter the generation or impact of ROS generation on cellular aging. Adapted from (Chan et al., 2010).

Autonomous pacemaking of SNc neurons relies on $Ca_v1.3$-channels, leading to a permanent overload of intracellular Ca^{2+} which cannot sufficiently be buffered by calcium binding proteins, like calbindin, due to less content in SNc neurons, thus excessive intracellular Ca^{2+} can lead to: 1) oxidative stress and mitochondrial dysfunction (see Figure 3-3); 2) Ca^{2+} can promote aSYN aggregation (Goodwin et al., 2013).

3.3.3 Calcium dysregulation leads to oxidative stress and mitochondrial dysfunction

In the past few decades, attention has turned to the role of mitochondrial dysfunction and oxidative stress as potential mechanisms involved in vulnerability to PD or in disease progression (Henchcliffe and Beal, 2008; Schapira, 2008; Vila et al., 2008).

Oxidative stress is thought to be the common mechanism that leads to cellular dysfunction in either familial or idiopathic PD. Generally, the brain consumes about 20% of the oxygen supply

of the whole body, and a considerable amount is converted to ROS (Kann and Kovacs, 2007). The excess production of ROS combined with relatively lowered cellular antioxidant activity cause oxidative stress in cells (Dias et al., 2013). The superoxide anion radical, the hydroxyl radical and hydrogen peroxide (H_2O_2) are ROS molecules (Gough and Cotter, 2011). Physiologically the peroxisomes are able to convert H_2O_2 to water by catalase, but when peroxisomes are damaged, H_2O_2 could be released into the cytosol which contributes significantly to the generation of oxidative stress (Dias et al., 2013). The link between oxidative stress levels and degeneration of SNc neurons is further supported by modeling the motor aspects of PD in animals using toxins which induce oxidative stress. 1-methyl-4-phenyl-1,2,3,6-tetrahydropyridine (MPTP), rotenone, and 6-hydroxydopamine (6-OHDA) are such toxins (Callio et al., 2005; Richardson et al., 2005).

The DA neurons are remarkably prone to oxidative stress because they harbor ROS-generating enzymes such as TH and MAO (Dias et al., 2013). Furthermore, excessive production of highly reactive hydroxyl radical ($^{\bullet}OH$) can result in tissue damage in nigral DA neurons due to the presence of "catalytic" iron (Halliwell, 1992). Because of this intrinsic sensitivity to ROS, a moderate oxidative stress can trigger a cascade of events that lead to cell demise (Hwang, 2013).

Mitochondrial dysfunction is another important source of oxidative stress associated with the pathogenesis of PD. Mitochondria are dynamic organelles with many functions, including energy generation, calcium homeostasis, stress response and cell death. Neurons depend on aerobic respiration via oxidative phosphorylation (OXPHOS) for the generation of adenosine triphosphate (ATP). Hydrogen peroxide and superoxide radicals are habitually produced in the mitochondria during OXPHOS as by-products (Winklhofer and Haass, 2010; Zhu and Chu, 2010).

Mitochondrial dysfunction was first linked to PD upon the recognition of MPTP-induced parkinsonism among some drug abusers, and selectively damaged cells in the SN were also detected through post-mortem analysis (Langston et al., 1983). Basically, any pathological situation leading to mitochondrial dysfunction can cause a dramatic increase in ROS and can lead to cellular damage and neurodegeneration (Zhu and Chu, 2010).

Excessive intracellular Ca^{2+} may also be involved in mitochondrial dysfunction through two mechanisms: firstly, an increase in intracellular Ca^{2+} levels caused by calcium dysregulation can have various effects on mitochondrial function. This includes changes in mitochondrial membrane potential, disruption of ATP synthesis, and generation of ROS, all of which can

contribute to oxidative damage and cell death (Nicholls, 2009; Starkov, 2008). Secondly, it can increase the intracellular NO level which can directly damage the neurons via nitrosylation of various proteins, and indirectly cell damage is led by peroxynitrite (NO_3^-) via activation of nitric oxide synthase (NOS) (Nicholls and Budd, 1998).

In addition, mutations in PD-related genes such as *LRRK2*, *Parkin* and *PINK-1* have been associated with calcium homeostasis and mitochondrial pathogenesis. For example, a study showed that modulation of LRRK2 through deletion, inhibition or mutagenesis of LRRK2 changed the mitochondrial Ca^{2+} efflux, which in turn lowered mitochondrial permeability transition pore (PTP) opening threshold and promoted cell death (Ludtmann et al., 2019). PINK-1 and PARKIN protect neurons from mitochondrial stress-induced dysfunction. After mitochondrial damage/dysfunction, PINK1 accumulates at the outer mitochondrial membrane (OMM) and recruits PARKIN from the cytosol to the OMM to remove the damaged mitochondria through autophagy, a process called mitophagy (Quinn et al., 2020). PINK1 deficiency causes mitochondrial accumulation of calcium, resulting in mitochondrial calcium overload (Gandhi et al., 2009).

Although mutations in genes associated with mitochondrial pathology can help us to better understand the process of the disease, it is still difficult to conclude that mitochondrial dysfunction is the root cause of Parkinson's disease because patients with these mutations tend to have a more severe and early-onset form of parkinsonism, which may not fully represent the complexity of Parkinson's disease in the population. Therefore, it is important to consider multiple factors when studying Parkinson's disease.

3.3.4 aSYN is a key protein involved in calcium dysregulation

Calcium ions may make important contributions to alpha synucleinopathies. *Rachel Lowe* et al. observed Ca^{2+} induced aSYN annular oligomers with atomic force microscopy (Lowe et al., 2004). Some *in vitro* studies found that Ca^{2+} can promote aSYN aggregates (Follett et al., 2013; Nath et al., 2011). On the contrary, raising the buffering capacity of Ca^{2+} can diminish the accumulation of aSYN (Rcom-H'cheo-Gauthier et al., 2017).

On the other hand, some studies have shown that aSYN can interact with intracellular Ca^{2+} stores and disrupt Ca^{2+} signaling in neurons. For example, Hettiarachchi et al. demonstrated that aSYN regulates Ca^{2+} entry pathways, and abnormal aSYN levels may consequently promote neuronal damage through dysregulation of Ca^{2+} homeostasis (Hettiarachchi et al.,

2009). Indeed, aSYN aggregates could activate calcium pump SERCA located in the endoplasmic reticulum and lead to calcium dysregulation (Betzer et al., 2018).

Although these studies showed that calcium dysregulation and aSYN aggregates have significant impacts in the pathogenesis of PD, none of them have provided any *in vivo* evidence, thus further investigation is needed to determine whether Ca^{2+} can trigger aSYN aggregates in animal models.

3.4 Mouse models used in PD research

3.4.1 The MPTP neurotoxin mouse model

Creating a perfect animal model of PD has been a big challenge, as the model needs to fulfil two very important conditions: the progressive degeneration of nigrostriatal neurons with subsequent decrease in DA and the formation of LB (aSYN pathology). Until now, none of the animal models were able to recapitulate all PD features, including the deterioration in behaviour and progressive aSYN pathology as well as the nigrostriatal degeneration. However, several models have been proposed which cover, to varying extents, some important PD features.

So far there are two types of experimental animal models: neurotoxic models and transgenic models. Most of the transgenic mouse models simulate familial form of PD, and only certain transgenic models displayed typical PD phenotypes, for example *LRRK2* and *PINK1* knockout mouse model. These two transgenic mouse models, however, do not show significant reduction of dopaminergic neurons and therefore may not be ideal animal models for PD. (Chia et al., 2020)

Apart from transgenic animal models, neurotoxins such as 6-hydroxydopamine (6-OHDA) and 1-methyl-4-phenyl-1,2,3,6-tetrahydropyridine (MPTP) are widely used for modelling PD. Compared to 6-OHDA, the MPTP model is able to mimic mitochondrial dysfunction and subsequent nigrostriatal neurodegeneration (inclusive DA decrease) and PD motor phenotypes in non-human primates, but fail to provoke formation of LB. MPTP toxicity in mice focuses on three types of cellular dysfunctions that may be important in the pathogenesis of PD: oxidative stress, mitochondrial respiration defect but low aSYN aggregation (Meredith et al., 2002). Although with limitations, this model establishes a standard not only for PD research but also

for preclinical evaluation of new therapies (Jackson-Lewis and Przedborski, 2007; Meredith and Rademacher, 2011; Schmidt and Ferger, 2001; Vila et al., 2000).

3.4.2 The $Ca_v1.3$ knockout model

In this model introduced by *Jörg Striessnig*, the L-type Ca^{2+} channels ($Ca_v1.3$) have been silenced by a fragment inserted into the calcium voltage-gated channel subunit α1D (*CACNA1D*) gene (Platzer et al., 2000). $Ca_v1.3$ $\alpha1D^{-/-}$ mice displayed normal sexual activity and reproduction and did not show any obvious anatomical abnormalities (Platzer et al., 2000). The knockout (KO) mice are neurologically normal with the exception of deafness, bradycardia and arrhythmia (Clark et al., 2003).

3.5 Aim of the study

As mentioned above, nigral DA neurons exhibit a continuous autonomous "pacemaking" activity that relies on $Ca_v1.3$-channels leading to increased calcium-related vulnerability of nigral DA neurons via oxidative stress, mitochondrial dysfunction and aSYN aggregation (Gleichmann and Mattson, 2011; Surmeier, 2018). It has been shown that reducing Ca^{2+} influx during "pacemaking" dramatically diminishes the sensitivity of SNc DA neurons to toxins used for generating animal models of PD. Back in the 1990s, *Kupsch* and colleagues demonstrated that treatment with nimodipine, a 1,4-dihydropyridine calcium channel blocker, can protect dopaminergic neurons against MPTP toxicity in animals (Kupsch et al., 1995; Kupsch et al., 1996). Accordingly, subsequent experimental studies have revealed that DHP inhibition of Ca_v1-channels by non-selective calcium-channel blockers (i.e., nimodipine or isradipine) may counteract these pathological cascades. In naïve mice, isradipine treatment decreased cytosolic calcium levels, diminished calcium-dependent mitochondrial oxidant stress, and normalized mitochondrial mass (Guzman et al., 2018). In a neurotoxic mouse model of PD, treatment with nimodipine was associated with attenuated mitochondrial dysfunction (Singh et al., 2016). Further, and most importantly, blockage of Ca_v1-channels with isradipine attenuated nigral DA-ergic cell loss in several neurotoxic mice models of PD by means of nigral neuroprotection (Chan et al., 2007; Ilijic et al., 2011; Wang et al., 2017).

Another study conducted in Denmark suggests a potential neuroprotective role in PD for centrally acting L-type Ca^{2+} channel blockers of the Dihydropyridine (DHPs) class (Ritz et al., 2010). Most recently, a double-blind, placebo-controlled clinical study led by the Parkinson

Study Group showed that 5 mg of immediate-release isradipine twice daily cannot slow early PD progression or provide protective benefit (Parkinson Study Group, 2020). Despite the disappointing result, the Ca^{2+} pathway still holds promise for further research.

The aim of the present study was to investigate whether there is a neuroprotective effect of Ca^{2+} channel knockout (KO) in a PD mouse model. For this purpose, $Ca_v1.3$ KO mice and C57BL/6J wild-type controls were used. The PD mouse model was introduced using chronic MPTP treatment, while saline-treated mice were used as controls.

To understand the molecular mechanisms underlying these findings, we investigated DA homoeostasis including dopamine, DOPAC and HVA, as well as the pattern of gene and protein expression of the important "players" regulating DA homoeostasis, namely: tyrosine hydroxylase (TH), dopamine transporter (DAT) and the major Lewy body component aSYN. The analyses were undertaken in the SNc as well as in the CPu.

4 Materials and Methods

4.1 Materials

4.1.1 Chemicals

NAME	ABBREVIATION	PROVIDER
acetamide		Sigma
agarose, LE		Seakem
ammonium Persulfate		Sigma
ethylenediaminetetraacetic acid	EDTA	Sigma
acetic acid		Roth
glycerol		Sigma
urea		Merck
potassium chloride	KCl	Merck
sodium chloride	NaCl	Merck
sodium hydroxide	NaOH	Merck
Orange G		Sigma
hydrochloric acid	HCl	Merck
SDS Ultra		Roth
Thio urea		Roth
tricine		Roth
Tris		Roth
Tris/HCL		Roth
Tween 20		Sigma
chlorophorm		Merck
ethanol		Merck
isopropanol		Merck
methanol		Merck
propanol		Merck
rotiload 1		Roth
tetramethylethylenediamine	TEMED	Roth
acrylamide		Serva
albumin bovine		Sigma
benzamidine		Sigma
1,4-Dithiothreit		Roth
ethidiumbromide		Serva

NAME	ABBREVIATION	PROVIDER
Gene Ruler 100bp DANN		Fermentas
Gene Ruler 1kp DANN		Fermentas
leupeptin		Roche
N,N-Methylene-bisacrylamid		Serva
Page Ruler protein marker		Fermentas
Trizol		Invitrogen

4.1.2 Devices

DEVICE	TYPE	PROVIDER
magnetic stirrer	7255	Eppendorf AG
micro centrifuge	5415-B-66696	Eppendorf AG
centrifuge	5810 R	Eppendorf AG
electrophorese	9601010	Biometra GmbH (1399)
freezer	14.879.673.5	Liebherr-Hausgeräte GmbH
shakers	503.470	IKA-Werke GmbH & Co.KG
refrigerated centrifuge	252326	Thermo Fisher Scientific
eppendorf gradient cycler		Eppendorf
power supply	Power pack P25	Biometra
sds page chamber	Mini 2-D cell	Biorad
autoclave	2540EL	Systec
laboratory balance	BP 2100	Sartorius
Real time cycler	Mx3000p	Stratagene
PCR cycler	T3 Thermocyler	Biometra
Gel imager		Syngene
Nanodrop spectrophotometer	ND1000	PeqLab
Microplate spectrophotometer		Biorad

4.1.3 Kits

NAME	PROVIDER
Taq DNA Polymerase	5 PRIME GmbH
dNTP Set dA, dC, dG, dT	Biomol GmbH
iScript™ cDNA Synthesis Kit	Bio-Rad

Power SYBR® Green PCR Master Mix (Applied Biosystems®)	Life Technologies
TURBO DNA-free™ (Invitrogen™)	Life Technologies

4.1.4 Antibodies

PRIMARY ANTIBODIES	SIZE OF ANTIGEN	HOST SPECIE	MANUFACTURER
α-Synuclein (D37A6)	18 kDa	Rabbit	Cell Signaling
β-Actin (C11)	43 kDa	Goat	Santa Cruz
TH (H-196)	60 kDa	Rabbit	Santa Cruz
DAT (AB1591P)	80 kDa	Rabbit	Millipore
SECONDARY ANTIBODIES	**ANTIGEN**		**MANUFACTURER**
Polyclonal goat-anti-rabbit Immunoglobulins/HRP	Anti - Rabbit		Dako
Polyclonal rabbit-anti-goat	Anti - Goat		Dako

4.1.5 Software

NAME	VERSION	PROVIDER
ImageJ	1.6	National Institutes of Health
AlphaEase	3.1.2	Alpha Innotech Corporation
GraphPad Prism	9	GraphPad Software Inc.
MxPro	v4.10	Agilent Technologies

4.2 Animals

The present study is based on experiments in MPTP-treated transgenic mice with $Ca_v1.3$ channel deficiency (voltage gated calcium channels of subtype 1.3). All animal experiments were performed in accordance with the European Communities Council Directive (63/2010/EU) and approved by LAGeSo Berlin (reference number G 0318/11) and were conducted by Ferry Sagala (PhD student Medical Neuroscience Program, Charité) from 2011 to 2013 under supervision of the project leader Daniel Harnack (MD, Department of Neurology,

Charité; currently Neurological Rehabilitation Clinic Beelitz-Heilstätten). Experimental procedures were carried out on male homozygous mice with a genetic deletion (knockout; KO) of $Ca_v1.3$ channels (kindly provided by DJ Surmeier, Chicago, IL) and their C57Bl/6J wild-type littermates. Backcrossing and genotyping were conducted as described previously (Sagala et al., 2012). Male $Ca_v1.3$ KO (n=16) and C57Bl/6J wild-type littermates (n=22), weighing between 20 and 28 grams, aged 2-3 months were used as experimental subjects (housing with free access to food and water at 21°C room temperature).

4.2.1 Study design

Animals were divided into four groups according to their genotype ($Ca_V1.3$ KO vs. WT) and the mode of treatment (placebo vs. MPTP). The numbers of mice used in this study were: WT-saline n=14, KO-saline n=8, WT-MPTP n=8, KO-MPTP n=8.

4.2.2 Genotyping

Genotyping was conducted by PCR from tail biopsies obtained from all experimental mice using primers as indicated in Table 4-1. Therefore, a quick NaOH DNA-extraction method was used. Accordingly, tail specimens were incubated with 600 µl of 50 mM NaOH at 95 °C for 30 min, neutralized with 50 µl of Tris–HCl (12.1 g/100 ml; pH 6.8), and finally centrifuged at 15,000 rpm for 6 min. The resulting supernatants were used to conduct PCR reactions.

Table 4-1 The primers for genotyping PCR

Target gene	Primer sequence	Size of product
WT ($Ca_v1.3+/+$)	5′-GCAAACTATGCAAGAGGCACC-3′	~180 bp
	5′-GGGAGAGAGATCCTACAGGTGG-3′	
KO ($Ca_v1.3-/-$)	5′-TTCCATTTGTCACGTCCTGCACCA-3′	~400 bp
	5′-GGGGTTATTGAGGGATAAACA-3′	
Slc25a21	5′-GAGACTCTGGCTACTCATCC-3′	~600 bp
(internal control)	5′-CCTTCAGCAAGAGCTGGGGAC-3′	

For each genomic PCR reaction, 5 µl genomic DNA was added to 20 µl Mastermix (15.05 µl ddH2O, 1.25 µl Mg-Acetate, 2.5 µl 10x reaction buffer, 0.5 µl DNTPs, 0.25 µl forward primer, 0.25 µl reverse primer and 0.2 µl Taq polymerase). The PCR was conducted using a PCR thermal cycler with the following parameters: (i) initial denaturation at 95 ºC for 5 min; (ii) 40 cycles of denaturation (95 ºC), annealing for 30s (56 ºC), and elongation for 60s at 72 °C; (iii)

the final elongation was conducted at 72 °C for 10 min. All PCR products were separated by 1.5% agarose gel electrophoresis at 120 V for 30 min in 1× TAE buffer and visualized with ethidium bromide by an UV photometer (see Figure 4-1).

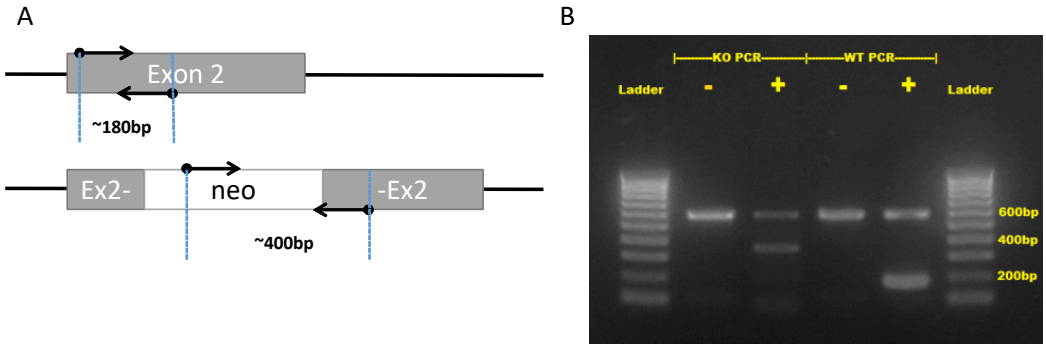

Figure 4-1 Genotyping of wild-type and $Ca_v1.3$ KO mice

(A) Target gene sequences of PCR primers, with amplification products of ~180bp size in WT gene and with 400bp size in KO gene. (B) $Ca_v1.3$ +/+ mice are WT mice with ~180bp and without ~400bp bands, while $Ca_v1.3$-/- mice are KO mice with ~400bp and without ~180bp bands; internal control gene (Slc25a21) PCR fragment is with size of 600 bp.

Amplification in the KO mice resulted in a Neo +/+ band (~400bps) with $Ca_v1.3$ -/-, which was specific in KO mice and thus not present in WT animals. For WT mice the PCR amplification resulted in a $Ca_v1.3$ +/+ band (~180bps) with Neo -/-. An internal PCR control which produced a ~600-bp band was used and proved to be present in all mice, indicating that the genotyping procedure *per se* was conclusive (see Figure 4-1). Using this method, mice could be sufficiently differentiated to their genotype, and based on these results mice were assigned either to be WT or $Ca_v1.3$ KO. After genotyping, 16 male $Ca_v1.3$ KO mice and 22 C57Bl/6J wild-type litters were eventually used for analysis. Only animals with a homozygous genotype were used for further experiments, because only in homozygous $Ca_v1.3$ -/- mice was the calcium channel completely diminished.

4.2.3 MPTP treatment and tissue preparation

Following a habituation period of two weeks, injections with MPTP (Sigma-Aldrich, Germany) were performed using a chronic dosage regime adapted to the protocol of Luchtman et al. (Luchtman et al., 2009) with some modifications due to an increased mortality rate in the MPTP cohort (Meredith et al., 2008). Thus, co-treatment with probenecid was omitted and the number of total injections per mice was reduced from ten to nine. A solution of MPTP hydrochloride

was administered intraperitoneally (i.p.) every 3.5 days at a dose of 20 mg/kg. All MPTP processing steps were done according to technical suggestions published elsewhere (Jackson-Lewis and Przedborski, 2007; Przedborski et al., 2001). Throughout the procedures, the investigator was blinded to the genotype of the mice. Saline (0.9%) was used to inject control mice. Four days after the last MPTP or saline injection, mice were sacrificed, and brains were snap frozen in nitrogen cooled 2-methylbutane (-40°C). Brain preparation was performed using a customized approach as reported previously (Sagala et al., 2012). In brief, cryostat sections of 1 mm thickness were taken from the caudate putamen (CPu, AP: +0.8 to -0.2 mm) and the midbrain containing the SNc (AP: -2.5 to -3.5 mm), according to the stereotaxic atlas of the mouse brain (Paxinos and Franklin, 2001) (cf. Figure 4-2). Further tissue preparation was performed on a freezing table (Leica, temperature set at -20°C) using a binocular loupe microscope (Leitz, Germany). From CPu containing brain sections, samples were taken from both hemispheres with a cannula (inner diameter 1.15 mm) and further processed for HPLC analysis. The residual striatum of each hemisphere was carefully dissected using a sharp edged 27-G-cannula as was done for the midbrain section comprising the SNc (Figure 4-2C). These brain samples were used for PCR and Western blot analyses.

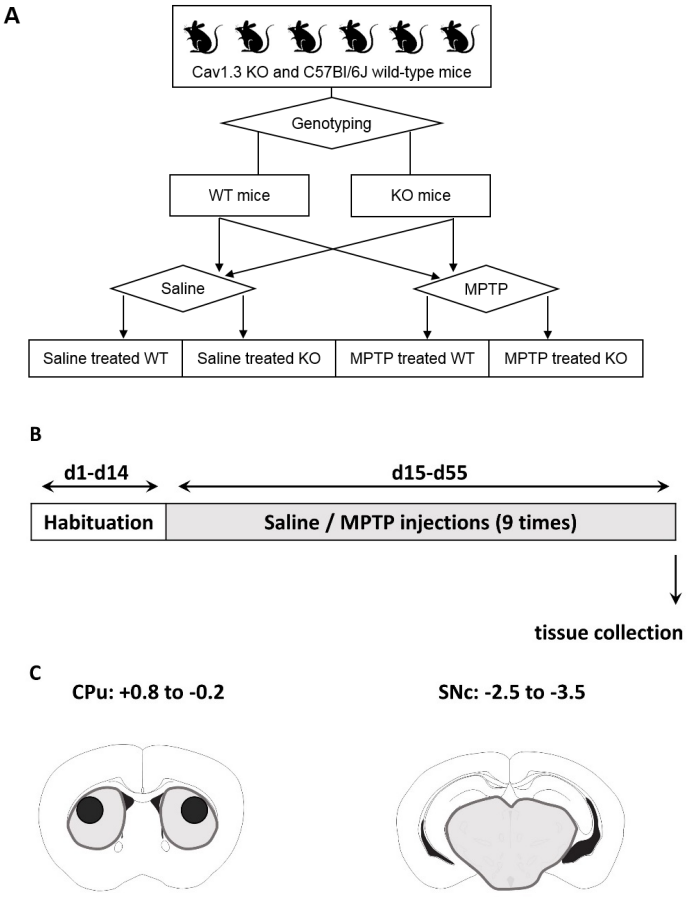

Figure 4-2 Flow chart detailing the experimental design.

A: $Ca_v1.3$ KO and C57BL/6J mice were used for this study. After genotyping, the mice were treated either with MPTP or with saline (as control group). B: Schematic drawing of the experimental design showing the schedule of MPTP injections following habituation of 2 weeks C: The anatomical regions used for biochemical analysis were CPu and midbrain comprising the SNc. For tissue preparation cryostat sections of 1 mm thickness were obtained from AP + 0.8 to -0.2 mm (for the striatum; CPu) and AP -2.5 to -3.5 mm (for the midbrain) according to the atlas of Paxinos & Franklin (2001). Tissue samples were dissected at the thick line (in grey) under optic control. Additionally, punches of ~1 mm diameter were taken from the dorsolateral striatum (black-filled circles) for HPLC analysis (for further details see text).

4.3 HPLC analysis of DA and its metabolites

Following appropriate tissue extraction (performed by the project leader Daniel Harnack, see above) the analysis of dopamine and its metabolites (dihydroxy-phenylacetate, DOPAC) and homovanillic acid, HVA) in striatal tissue samples was assessed by Ferry Sagala (see above) using HPLC and electrochemical detection (ED).

After sonication of striatal samples in perchloric acid, 50 µl of the homogenate were removed and added with an equal volume of 1 M sodium hydroxide solution for protein determination

using bicinchoninic acid (BCA) protein assay. Following centrifugation (14,000 rpm for 15 minutes at 4 °C), the supernatant was separated for HPLC-based analysis of monoamines (50 µl) as described previously (Sagala et al., 2012). Briefly, the extracts were separated on a column (Luna 5µ C18 (2); length: 150 mm; inner diameter: 2 mm; Phenomenex®, Aschaffenburg, Germany) at a flow rate of 0.3 ml/min. The mobile phase consisted of 80 mM sodium dihydrogene phosphate, 0.9 mM octane-1-sulfonic acid sodium salt, 0.5 mM ethylene-diamine-tetra-acetic acid disodium salt, 1.28 mM phosphoric acid, and 5% 2- propanol (all chemicals from Merck KGaA, Darmstadt, Germany). Monoamines were detected using an electrochemical detector (Decade, ANTEC Leyden BV, Leiden, The Netherlands) at an electrode potential of 0.6 V. For calibration, a perchloric acid standard mixture of known concentration (1 µM for DA and 0.1 µM for DOPAC and HVA) was measured before and after analyzing all samples of each brain. Sample analysis was performed based on peak areas using a computer-based chromatography data system (Class-VP, Shimadzu Deutschland GmbH, Duisburg, Germany) in relation to the mean of the applied calibration solutions. Tissue levels of all neurochemicals are represented as nanomolar per gram (nmol/g) protein.

4.4 Gene expression analysis

4.4.1 Extraction of RNA with Trizol®

The Trizol® protocol was used to extract RNA and protein from the same brain sample. 1 ml TRIzol® reagent was added to each sample followed by an incubation time of 5 minutes at room temperature which allowed the complete dissociation of nucleoprotein complexes. Thereafter, 0.2 ml of chloroform per 1 ml of TRIzol® reagent was added. The tubes were shaken vigorously by hand for 15 s and incubated at room temperature for 2 minutes. The samples were then centrifuged at 12,000 rpm for 15 minutes at 4°C followed by a transfer of the aqueous phase to new Eppendorf™ tubes. The RNA was precipitated from this aqueous phase by addition of 0.5ml of isopropanol. This mixture was centrifuged for 30 minutes at 12,000 rpm at 4°C so that the RNA precipitate formed a gel-like pellet at bottom of the tube. After removing the supernatant, the RNA pellet was washed once with 1ml 75% ethanol. The sample was inverted, mixed briefly and centrifuged at 12,000 rpm for 30 minutes at 4°C. Finally, the RNA pellet was air dried for 5-10 minutes and dissolved in 40µl RNase-free water by passing the solution through the tip of the pipette for a few times and incubating for 10 minutes at 55 to 60°C. The RNA samples were then stored at -70°C.

4.4.2 The quality of the purified RNA

The high quality of the extracted RNA from all samples was assessed by measuring the optical density (OD) of the samples and by gel electrophoresis.

The absorption maximum of RNA was at 260 nm, while the absorption maximum of DNA was at 280 nm. The ratio of the absorbance between 260 and 280 nm was used to assess whether the RNA was well purified of any DNA contaminants. Thus, a value of 1.8-2.0 was indicative for pure RNA, which was the case for the samples prepared from CPu and midbrain samples (Table 4-2).

Table 4-2 The RNA quantity and quality as measured by the Nanodrop photometer

BRAIN AREA	RNA concentration [ng/µL] Mean ± SD (Min, Max)	OD260/OD280 Mean ± SD (Min, Max)
CPu	269.6 ± 43.82 (185.7-353.2)	1.92 ± 0.040 (1.84-1.98)
SNc	415.9 ± 79.23 (309.08-638)	1.95 ± 0.042 (1.82-2.05)

After successful purification, the RNA was reversely transcribed to cDNA, which was then used for any downstream gene quantification analysis.

Furthermore, prior to this procedure the primer efficiency was measured during PCR runs using cDNA dilution series in a self-designed manner. The C_t-values of each dilution step were determined in triplicates for each primer. The resulting graphs allowed the determination of their respective increment using the formula $C_T = m(\log \text{quantity}) + b$.

The increment in turn allowed the calculation of the primer efficiency using the formula $E=10^{-1/a}$. The calculation was done automatically with the qPCR software.

Results of qPCR with cDNA dilution series using 18s RNA (reference gene), aSYN, DAT and TH primers are shown in Table 4-3.

Table 4-3 An overview of efficacy and coefficients of the primers designed

18s RNA Y = -3.356*LOG(X) + 15.99, Eff. = 98.6% R^2:0.994
α-Synuclein Y = -3.416*LOG(X) + 20.97, Eff. = 96.2% R^2: 0.999
DAT Y = -3.252*LOG(X) + 28.02, Eff. = 103.0% R^2:0.999
TH Y = -3.107*LOG(X) + 27.54, Eff. = 109.8% R^2:0.996

The mean C_t-values determined for each cDNA dilution step were registered on the Y-axis. The logarithms of the respective cDNA concentrations (log(c)) were plotted on the x-axis. As a result, the determination coefficients (R2) were always >0.99, indicating an almost linear correlation between the coordinate pairs determined by the logarithm of a given cDNA concentration and the respective C(t)-value.

Employing the above-mentioned formula, efficacy values for the self-designed primers were found to range from 96.2% to 109.8%, indicating excellent primer performances.

The melting curve was also run after the qPCR amplification to verify that only one single product has been amplified. Melting curve analysis showed there were no unspecific amplicon (e.g., gDNA) identified and no amplicon was detected in any template control (NTC) samples, which means the qPCR was conducted as expected (data not shown).

4.4.3 Real-time PCR for gene expression analysis

4.4.3.1 RNA extraction and quantification

The RNA was extracted using the TRIzol reagent according to the manufacturer's instructions (Invitrogen™), as described above. The concentrations of RNA samples were determined with the Nanodrop UV spectrophotometry (ND-1000). A ratio between 260/280 nm was calculated and a ratio ≈ 2 is generally accepted as "pure" for RNA. For quality control 1 µl RNA was mixed with 6 µl ddH_2O and 3 µl of RNA buffer (containing ethidium bromide) followed by incubation for 5 min at 60 °C. The RNA products were separated in 1% agarose gel electrophoresis at 120 V for 30 min in 1× TBE buffer and visualized with ethidium bromide with a UV photometer. RNA of good quality normally showed two sharp bands for the 28S and 18S ribosomal RNA.

4.4.3.2 DNAse treatment

5 µg RNA (obtained from the above-mentioned protocol) was mixed with 5 µl 10x DNAse-buffer, 1µl DNAse, and the final volume was set to 50 µl with ddH_2O. The mixture was incubated at 37°C for 30 min and the reaction was stopped by adding 5 µl of inactivation reagent. The mix was then centrifuged for 5 min at 10,000 rpm and the supernatant containing the purified RNA was used later.

4.4.3.3 cDNA synthesis

After the DNA digestion process, the RNA was reverse-transcribed into cDNA with iScript™ cDNA Synthesis Kit according to the manufacturer's instructions. Briefly, 10µL DNAse-treated RNA was mixed with 4µL 5x reaction mix, 1µL reverse transcriptase enzyme and 5µL ddH_2O (total volume 20µL). The RT-PCR program was set to: initial reaction at 25°C for 5 min followed by double strand synthesis at 42°C for 30m and inactivation of the reaction at 85°C for 5 min. Aliquots of the cDNA were adjusted to 1ng/ µL and were stored at -20°C until later use.

4.4.3.4 Primer design

In order to measure the gene expression of aSYN, TH and DAT according to the SYBR Green-based qPCR protocol, appropriate primers were designed (see Table 4-4).

The following general guidelines were used to design primers:

- Size of amplification product: 75-200bp
- Avoiding regions and primers which have secondary structures
- Avoiding regions and primers with long repeats of single bases
- GC content of primers 50-60%
- Primer melting (annealing) temperature T_m near 60°C

Table 4-4 qPCR primers designed to quantify 18s RNA, SNCA, TH and DAT

Gene	F/R	Primer sequence	Product size
Mouse 18s RNA	Forward	5' - GTAACCCGTTGAACCCCATT	151 bp
	Reverse	5' - CCATCCAATCGGTAGTAGCG	
Mouse SNCA	Forward	5' - GGGAGTCCTCTATGTAGGTTCC	97 bp
	Reverse	5' - TCCAACATTTGTCACTTGCTCT	
Mouse TH	Forward	5' - CCAAGGTTCATTGGACGGC	137 bp
	Reverse	5' - CTCTCCTCGAATACCACAGCC	
Mouse DAT	Forward	5' - TGGCTTCGTTGTCTTCTCCT	164 bp
	Reverse	5' - GCATGAGGAAGAAGACAGCG	

4.4.3.5 PCR for primer quality control

In order to verify the specification of designed primers, PCR was conducted from cDNA and the size of the amplified target was controlled by electrophoresis. For PCR 2.5 µl cDNA were mixed with 1 µl DNTPs, 1 µl forward primer, 1 µl reverse primer, 0.25 µl taq polymerase, 1.25 µl $MgCl_2$, 2.5 µl 10x reaction buffer and 15.5 µl ddH_2O. The parameters for PCR reaction were:

- Initial denaturation at 94 ºC for 2 min
- 39 cycles of denaturation (94 ºC, 30s), annealing (65 ºC, 30s), and elongation (72 °C, 30s)

The PCR amplification products were separated using a 2% agarose gel electrophoresis (with ethidium bromide) at 80V for 40 minutes. After electrophoretic separation, the gels were photographed under UV light.

4.4.3.6 Preparation of cDNA pools for real time PCR

Gene quantification was performed by normalizing it to 18s RNA gene and by a standard curve derived from sample pools with different concentrations. A dilution series of five pools with a ratio of 1:5 was used (see Table 4-5; Pool 1: 5ng/µL; Pool 2: 1ng/µL; Pool 3: 0,2ng/µL; Pool 4: 0,04ng/µL; Pool 5: 0,008ng/µL).

Table 4-5 Preparation of cDNA pools

Pool	cDNA concentration	cDNA volume for PCR (µL)	Final cDNA amount (ng)
Pool 1	5	5	25
Pool 2	1	5	5
Pool 3	0.2	5	1
Pool 4	0.04	5	0.2
Pool 5	0.008	5	0.04
Unknown Sample	1	5	5

4.4.3.7 Quantitative real time PCR (qPCR) and relative gene expression

SYBR Green fluorescence is significantly increased when binding to double-stranded DNA. During the repeated extension phases, more and more SYBR Green bind to the PCR product, resulting in an increased fluorescence. Consequently, during each subsequent PCR cycle, more fluorescence signal is detected.

For the present study the relative gene expression of aSYN, DAT and TH among four animal groups were determined with qPCR. The cycle threshold (C_t)-values were determined in triplicates, both for target genes and 18s RNA which served as reference gene. In the same run, five sample pools were amplified with both target gene and reference gene primers. This allowed a standard curve for quantification of genes of interests in unknown samples. The following table shows the composition and the conditions for qPCR runs (see Table 4-6).

Table 4-6 Composition of qPCR reactions and reaction conditions

Composition of qPCR reaction			
Power SYBR Green PCR Master Mix	12.5 µl		
Primer 1	0.75 µl		
Primer 2	0.75 µl		
ddH_2O	6 µl		
cDNA template	5 µl		
qPCR reaction conditions			
Pre-treatment	50 °C	2 min	1 cycle
Initial denaturation	95 °C	10 min	1 cycle
Denaturation	95 °C	15 sec	40 cycles
Annealing	60 °C	30 sec	
Extension	72 °C	30 sec	
Melting curve			
95 °C	1 min		
55 °C	30 sec		
95 °C	30 sec		

qPCR analysis was performed with the software MxPro v4.10. The relative gene expression (R) was determined using the efficiency-corrected method (Pfaffl):

$$R = \frac{(E_{target\ gene})^{\Delta Ct\ target\ gene\ (control\text{-}stimulated\ sample)}}{(E_{housekeeping\ gene})^{\Delta Ct\ housekeeping\ gene\ (control\text{-}stimulated\ sample)}}$$

4.4.3.8 Determination of standard curve and primer efficacy

The cycle threshold (C_t)-values were determined in triplicates. The five pre-determined concentrations (i.e. the pool samples of cDNA) were logarithmically plotted as x-axis and the corresponding mean C_t-values were plotted as y-axis variable. The resulting standard curve allowed the determination of cDNA concentration in an unknown sample using the following equation: C_T = m(log quantity) + b, where m is the slope and b is the intercept. The efficacy of the designed primers (E) was calculated according to the equation $E=10^{-1/a}$

4.5 Protein expression analysis

4.5.1 Protein isolation and quantity measurement

4.5.1.1 Protein precipitation

Isopropanol was added into the tube in which the organic (phenol-chloroform) phase remained during the RNA extraction process (see above). Thereafter, samples were incubated for 10 minutes for the initial homogenization. After this step, the samples were centrifuged at 12,000 rpm for 10 minutes at 4°C and the supernatant was carefully removed and discarded from each tube. The remaining protein pellets then proceeded to the protein washing step. A washing solution (0.3 M guanidine hydrochloride in 95% ethanol) was added to the tube which was then incubated for 20 minutes at room temperature. The samples were centrifuged at 7,500 rpm for a further 5 minutes at 4°C after which the washing solution was discarded. This rinsing step was repeated three times. Finally, 100% ethanol was added to the protein pellet after the third wash and the samples were incubated for 20 minutes at room temperature followed by centrifugation at 7,500 rpm for 5 minutes at 4°C. After removing the ethanol, the protein pellet was air dried for five minutes. The re-suspension solution was prepared, and the protein re-suspension step was carried out.

4.5.1.2 Re-suspension solution

In our pilot experiment, 1% SDS was used as re-suspension solution according to the TRIzol® protocol. However, the soluble capability of SDS solution and the yield concentration were not satisfactory. Thus, urea buffer was taken as suspension solution (see Table 4-7).

Table 4-7 Composition of urea protein resuspension solution

	Concentration	Molarity	Weight/Volume
Tris/HCl	25mM	157.6	394 mg
KCl	50mM	74.6	373 mg
EDTA	3mM	292.3	87.7 mg
Benzamidin	2.9mM	120.2	34.8 mg
Leupeptin	2.1µM	463	0.09 mg (19µL from 5mg/ml)
urea	7 M	60.1	840 mg
thiourea	2 M	76.1	240 mg
Water	-	-	100 µL
DTT	70 mM	154.2	100 µL from 1.4M

4.5.1.3 Protein concentration measurement

Protein concentration was determined according to the Bradford method. Standard solutions of bovine serum albumin (BSA) of 200, 100, 50, 10 µg/ml were prepared, and unknown samples were diluted 1:100. 50 µL of each sample (either standard or sample) were mixed with 200 µl Bradford solution and incubated 10 minutes in darkness. Water was used as negative control and each sample (water, standard or sample) was measured in triplicates. The absorbance at 595 nm was measured. A standard curve of absorbance versus BSA protein was prepared, and the protein amounts in the unknown samples were estimated from the standard curve.

4.5.1.4 The quantity and quality of extracted proteins

The TRIzol protocol was used to extract both proteins and RNA from brain tissue samples. The amount of protein in each sample was quantified using the Bradford protocol and respective values are given in table 4-8.

Table 4-8 An overview of protein concentrations determined in SNc and CPu

Brain Area	Protein Concentration µG/µL (Mean ± SD, min-max)
SNc	1.94 ± 0.284 (1.291 -- 2.362)
CPu	0.84 ± 0.119 (0.560 – 1.046)

The TRIzol manufacturer's instruction protocol was modified at the step of the re-suspension of the protein pellet to support the efficient re-solubilization of proteins not only by denaturing conditions (7 M urea), but also by facilitating the reconstitution of hydrophobic protein

sequences and transmembrane proteins (2 M thiourea). Thiourea is a non-chaotropic compound which is frequently used in PAGE applications due to its high capacity to re-solubilize membrane proteins. DTT is widely used to reduce the disulfide bonds of proteins and, more generally, to prevent intramolecular and intermolecular disulfide bonds from forming between cysteine residues of proteins. Due to the strong denaturing conditions used, this protocol is well suited for protein studies, including protein quantitation, and the TRIzol extraction method generated sufficient protein amounts for the intended immunoblotting experiments.

4.5.2 Tricine-SDS-Page and Western blot

4.5.2.1 Tricine-SDS-Page

Ten µg of each sample were prepared by adding 1 volume 4x Reducing Laemmli Buffer (Roti-Load). The mixture was incubated for 5min at 95°C, cooled down to room temperature (RT) and then used for the next step.

Table 4-9 Solutions and buffers used to cast Tricine gels

AB-3 solution	**Gel buffer 3x. pH 8.45**
48g Acrylamide	363.42g Tris
1.5g Bisacrylamid	145.84g or 130mL 25%HCl
Fill to 100mL and store at -20°C	3g SDS
-	Fill to 1L and store at RT
10% separating gel solution	**4% stacking gel solution**
6mL AB-3	1mL AB-3
10mL 3x gel buffer	3mL 3x gel buffer
3g glycerol	-
11mL water	8mL water
150µL 10% APS	90µL 10% APS
15µl TEMED	9µL TEMED

Glass plates were cleaned carefully with water followed by 70% ethanol. Two glass plates were in the clamp assembly and transferred to the casting slot in which 10-11mL of separating gel solution was pipetted. After adding 1mL 70% ethanol onto the separating gel, its polymerization was conducted for 30min at room temperature before the ethanol layer was discarded carefully and thoroughly. Stacking gel solution was added and a sample comb was inserted immediately

between the glasses. Stacking gel was polymerized for one hour at RT. Table 4-9 gives an overview of the solutions and buffers used for the gels.

Glass plates were placed in the buffer chamber. The cathode buffer was added as the upper buffer and the anode buffer as the lower buffer (see Table 4-10). Combs were removed carefully, and wells were washed with the cathode buffer. Afterwards, samples were loaded, and protein standard marker was also used. The voltage was set to 40V for 20min followed by 3 hours at 100V.

Table 4-10 Composition if cathode and anode buffers used during Tricine-SDS-Page

10x cathode buffer, pH8.25	**10x anode buffer, pH8.9**
121.14g Tris	121.14g Tris
179.2g tricine	32.81g or 29.3mL 25%HCl
10g SDS	-
Ad 1L and store at RT	Ad 1L and store at RT

4.5.2.2 Immunoblotting and relative protein quantification

After electrophoresis the gels were carefully removed from the plates and incubated for 5 min in transfer buffer (see Table 4-11). Two pieces of Whatman paper were cut (6x9 cm) and incubated in transfer buffer. The same cutting was done for a PVDF membrane which was also transferred to transfer buffer following incubation in methanol for one min. One layer of the Whatman paper was put on the plate of a semi-dry blotting cassette, followed by one layer of PVDF membrane, the gel and the second layer of the Whatman paper (each one by one). Air bubbles were carefully removed by rolling over the sandwich. The intensity of the electric field was set to 0.4mA/cm^2 and the transfer was conducted overnight at 4°C.

Table 4-11 Composition of transfer buffer and washing solutions used during immunoblotting

1xTransfer buffer, pH 8.6
36.34g Tris
6g or 5.7mL 100% acetic acid
Ad 1L and store at RT
10xTBS
24.4g Tris
80g NaCl
Adjust pH to 7.6 with 25%HCl (ca.20mL)
Ad 1L and store at RT
1xTBS 0.2% Tween (TBS-T)
100mL 10xTBS
Ad 1L Dest Water
Ad 2mL Tween and store at RT
4% BSA/TBS-T
4 g BSA
Ad 100 mL TBS-T

After immunoblotting, membranes were incubated for 5min at RT in TBS-T (see Table 4-11). Each membrane was incubated for 1h and at RT in 4% BSA/TBST and then incubated overnight at 4°C in primary antibody diluted in 4% BSA/TBS-T. Following rinsing 3x10min in TBS-T, membranes were incubated with an appropriate secondary antibody diluted in 4% BSA/TBS-T each at room temperature. After the membrane was washed for additional 3x10min with TBS-T at RT, the membrane was overlaid with 1mL ECL solution and incubated for 1min. The membrane was placed in a specific cassette and chemiluminescent signals were detected on hyperfilms (Kodak) and scanned as JPG files with a resolution of 150 dpi. The chemiluminescent signals were quantified using the ImageJ software. Primary and secondary antibodies used are listed in table of antibodies).

4.6 Statistical Analysis

Statistical analyses were conducted using GraphPad Prism (version 6.00; GraphPad Software Inc., La Jolla, CA, USA). Tissue levels of all neurochemicals (HPLC) were represented as

nanomolar per milligram (nmol/mg) protein. Values of Western blot and qPCR were relative quantification as saline treated WT mice group was set as 1, and the expressions of Western blot and qPCR were confirmed as Gaussian (D'Agostino and Pearson omnibus test) and analysed by parametric statistics (unless otherwise stated) using factorial analysis of variance (two-way ANOVA) and appropriate post-hoc (t-test; Bonferroni corrected) two-tailed tests (for details, see Results). The null hypothesis was accepted for $\alpha < 0.05$ and only significant terms are given in the text. All data are plotted as group mean and standard error of mean (S.E.M.), and genotype and treatment were set as variable factors for ANOVA testing.

5 Results

The results focus on three parts: The effects of chronic MPTP treatment in $Ca_v1.3$ KO and wild-type mice on

a) tissue levels of striatal dopamine and its metabolites
b) gene expression of aSYN, TH and DAT
c) protein expression of aSYN, TH and DAT

The tissues for HPLC analysis were taken from CPu containing brain sections in both hemispheres with a cannula (inner diameter 1.15 mm) and further processed for HPLC analysis. After that, the residual striatum of each hemisphere and midbrain section containing SNc were carefully disserted for further PCR and Western blot analysis.

5.1 Dopamine and its metabolites

The tissue levels of monoamines (DA) and their respective metabolites dihydroxy-phenylacetate (DOPAC) and homovanillic acid (HVA) were measured by HPLC and electrochemical detection (ED).

Chronic MPTP treatment resulted in a significant decrease of striatal DA to 32.8% ± 15.1% (mean and S.E.M) in wild-type mice and to 50.4% ± 10.0% in $Ca_v1.3$ KO mice, each in comparison to saline-treated controls with the corresponding genotype (MPTP effect: F1.23 120.1, $p<0.0001$, Figure 5-1A). Importantly, the decrease of striatal DA was significantly less pronounced in $Ca_v1.3$ KO mice (interaction effect MPTP x genotype: F1.23 4.302, $p<0.05$), emphasizing that $Ca_v1.3$ channel deficiency attenuates MPTP induced DA depletion. Chronic MPTP treatment was also followed by a significant reduction of DA-ergic metabolites DOPAC and HVA: levels of DOPAC (Figure 5-1B) decreased to 47.4% ± 12.0% in wild-type and to 50.0% ± 6.7% in $Ca_v1.3$ KO mice (MPTP effect: F1.23 56.18, $p<0.0001$), whereas the tissue contents of HVA (Figure 5-1C) were diminished to 48.1% ± 6.9% in wild-type and to 55.7% ± 7.5% in $Ca_v1.3$ KO mice (MPTP effect: F1.23 34.44, $p<0.0001$), as compared to respective saline-treated controls.

Regarding the striatal DA turnover (given by the ratio of DA-ergic metabolites to DA), a significant increase was only seen in wild-type mice (~156.7% ± 7.2%) but not in $Ca_v1.3$ KO mice (~110.6% ± 6.2%), each in comparison to saline-treated controls with the corresponding genotype (MPTP effect: F1,23 12.46, $p<0.005$ and interaction effect MPTP x genotype: F1.23 5.554, $p<0.05$, Figure 5-1D). Importantly, only in MPTP-treated KO mice was the DA turnover unaffected (see Bonferroni post-test, Figure 5-1D).

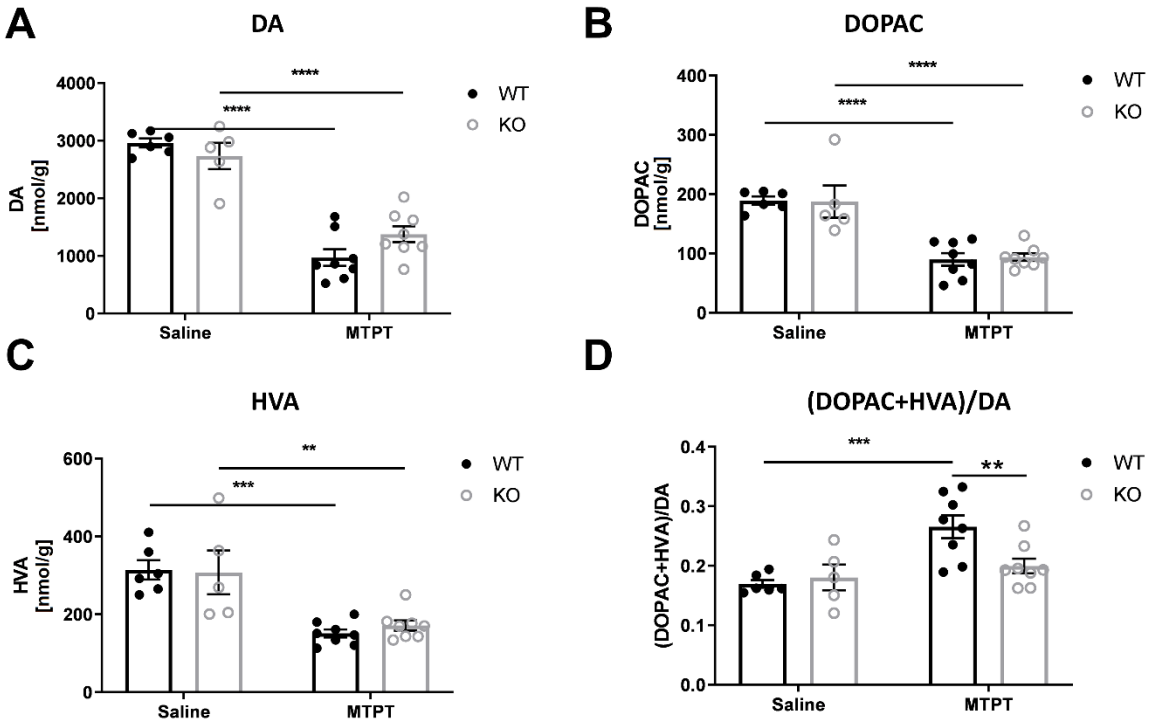

Figure 5-1 HPLC analysis showed a relative neuroprotective effect on residual DA levels

HPLC analysis for DA (A) and its metabolites DOPAC (B) and HVA (C) each in nmol/g protein, as well as for DA turnover (DOPAC+HVA)/DA (D) for saline and MPTP-treated mice of both genotypes (wild type in black and transgenic $Ca_V1.3$ -/- mice in grey). All values are shown as group mean and S.E.M. The most important findings were a less decrease of DA in $Ca_V1.3$ -/- mice and a concomitant decreased DA turnover.

(A) Chronic MPTP treatment resulted in a significant decrease of striatal DA and the decrease of striatal DA was significantly less pronounced in Cav1.3 KO mice (ANOVA MPTP $p < 0.0001$, genotype n.s., MPTP x genotype $p < 0.05$). (B, C) Chronic MPTP treatment was also followed by a significant reduction of DA-ergic metabolites DOPAC and HVA: (B) ANOVA MPTP $p < 0.0001$, genotype n.s., MPTP x genotype n.s. (C) ANOVA MPTP $p < 0.0001$, genotype n.s., MPTP x genotype n.s. (D) For the striatal DA turnover, (DOPAC+HVA)/DA, a significant increase was only seen in wild-type mice but not in Cav1.3 KO mice, ANOVA MPTP $p < 0.01$, genotype n.s., MPTP x genotype $p < 0.05$.

Bonferroni post-test was conducted within the same genotype (**** $p<0.0001$, *** $p<0.001$, ** $p<0.01$ vs. saline-treated) and within the same treatment group (** $p<0.01$ vs. wild type).

5.2 Gene expression analysis

In the antecedent animal study, mice of both genotypes (WT vs. $Ca_v1.3$ KO) were treated with 9 consecutive i.p. injections of either MPTP (treatment group) or saline (control group). All mice were sacrificed at the age of 51 – 55 days. The gene expressions of all surrogate markers (*SNCA*, TH, VMAT and DAT) were assessed by qPCR for which the reference value was set as 1 in saline treated WT mice. Values outside the range of ± 2x standard deviations were considered outliers and were excluded from analysis.

5.2.1 Relative gene expression of aSYN (*SNCA*)

As shown in Figure 5-2 the expression levels of the alpha synuclein gene *SNCA* was similar for saline and MPTP-treated animals irrespective of their genotypes. Moreover, there were no significant differences for the *SNCA* gene expression in the two target areas CPu and midbrain. Taken together, there were no significant interactions, i.e., treatment or genotype effects among the four groups in brain samples of SNc, and *SNCA* m-RNA was expressed at comparable levels between genotypes.

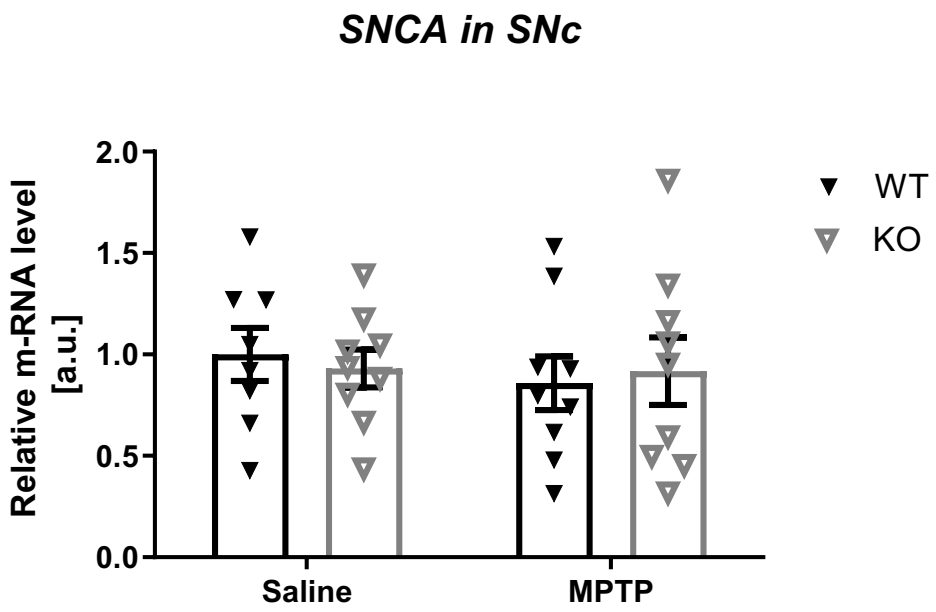

Figure 5-2 Relative gene expression of aSYN (*SNCA*) in SNc remained unchanged following MPTP

SNCA was measured in SNc brain samples from WT (black bars) and $Ca_v1.3$ KO mice (grey bars), treated with either saline or MPTP, using qPCR. All values are shown as group mean and S.E.M. ANOVA: MPTP ns, genotype ns, MPTP x genotype ns.

5.2.2 Relative gene expression of *TH*

Chronic MTPT treatment diminished the levels of *TH* mRNA in the midbrain, both in wild-type and in $Ca_v1.3$ KO mice (MPTP effect: $F_{1,30}$ 24.23, $p < 0.0001$, see Figure 5-3), and this reduction was less pronounced in $Ca_v1.3$ KO mice by means of a significant interaction effect (MPTP x genotype: $F_{1,30}$ 4.721, $p < 0.05$). Referring to this, it is important to note that in saline-treated $Ca_v1.3$ KO mice (control group) the *TH* mRNA expression *per se* was diminished in comparison to wild-type animals, which was so far unknown. Remarkably, saline-treated $Ca_v1.3$ KO mice had lower *TH* gene levels compared to WT mice in nigral samples (see Figure 5-3: asterisks for Bonferroni corrected t-tests). MTPT treatment *per se* reduced the *TH* gene levels in the SNc, both in WT and $Ca_v1.3$ KO mice to similar expression levels.

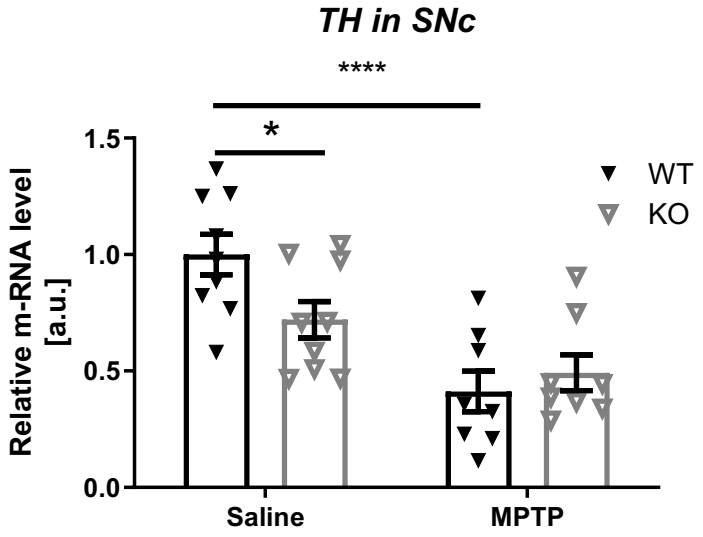

Figure 5-3 Relative gene expression of *TH* in SNc demonstrated an overall reduction in all mice undergoing MPTP treatment with less reduction in $Ca_v1.3$ KO mice

TH was measured in nigral (SNc) brain samples from WT (black bars) and $Ca_v1.3$ KO mice (grey bars), treated with either saline or MPTP, using qPCR. *: $p < 0.05$ for genotype effect for KO vs. WT mice, both treated with saline. *: $p < 0.05$ and ****: $p < 0.0001$ for treatment effect of MPTP-treated vs. saline treated WT mice. All values were shown as group mean and S.E.M. ANOVA MPTP $p < 0.0001$, genotype n.s., MPTP x genotype $p < 0.05$.

5.2.3 Relative gene expression of *DAT*

Chronic MPTP treatment significantly decreased nigral *DAT* mRNA only in wild-type mice, while the expression level of DAT mRNA in MPTP treated $Ca_v1.3$ KO, in contrast, remained unaffected compared to saline-treated controls (see Figure 5-4; MPTP effect: F1.28 5.79, $p < 0.05$ and interaction effect MPTP x genotype: F1.28 5.40, $p < 0.05$). These results were linked to a significant decrease of striatal DAT protein expression (see Figure 5-7, MPTP effect: F1.30 15.78, $p < 0.001$), which was visually more pronounced in wild-type mice.

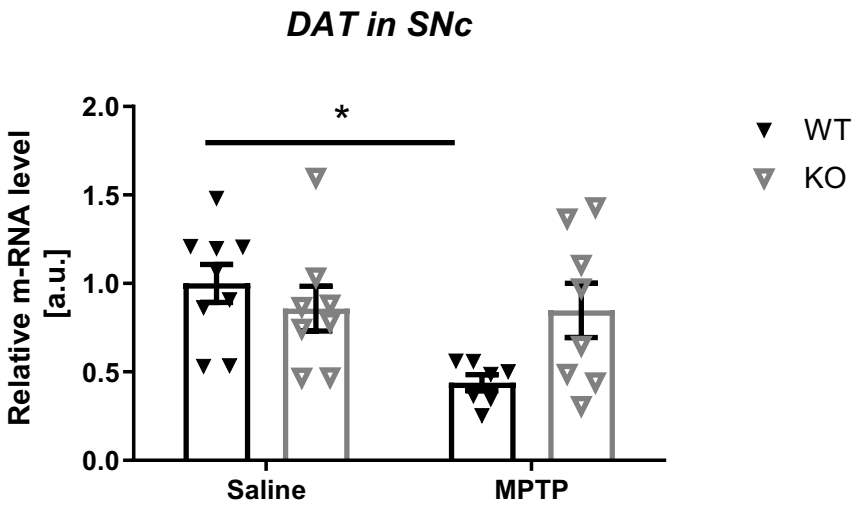

Figure 5-4 Relative gene expression of *DAT* in SNc showed a significant preservation of DAT mRNA in midbrain samples of $Ca_v1.3$ KO mice

DAT was measured in SNc brain samples from WT (black bars) and $Ca_v1.3$ KO mice (grey bars), treated with either saline or MPTP, using qPCR *: $p < 0.05$ for treatment effect of MPTP-treated vs. saline treated WT mice. All values are shown as group mean and S.E.M. ANOVA MPTP $p < 0.05$, genotype n.s., MPTP x genotype $p < 0.05$.

5.3 Protein expression analysis

As for the protein analysis, saline-treated WT mice were assessed as reference with a value of one. For all experimental groups, the protein β-Actin was used as an internal control. Protein expression was performed by immunoblotting whereby quantitative values were obtained by measuring the optical density of each band using the image analysis software ImageJ described above (see Materials and Methods).

5.3.1 Relative protein expression of aSYN

The relative amount of aSYN in brain samples of the SNc and CPu for the different experimental groups is shown in Figure 5-5. Using the appropriate antibody against aSYN, a specific signal for aSYN with a relative mobility of 19 kDa could be detected (Figure 5-5C and 5-5D).

As shown in Figure 5-5, following chronic MPTP treatment, aSYN protein expression was increased in both genotypes in the substantia nigra (Figure 5-5A, MPTP effect: F1.28 16.25, $p < 0.001$) and in the striatum (Figure 5-5B, MPTP effect: F1.31 16.91, $p < 0.001$). Most importantly, the protein expression of aSYN was significantly higher in MPTP-treated WT mice when compared to $Ca_v1.3$ -/- mice ($p < 0.05$). Saline-treated mice of both genotypes had similar aSYN levels, both in SNc and in CPu.

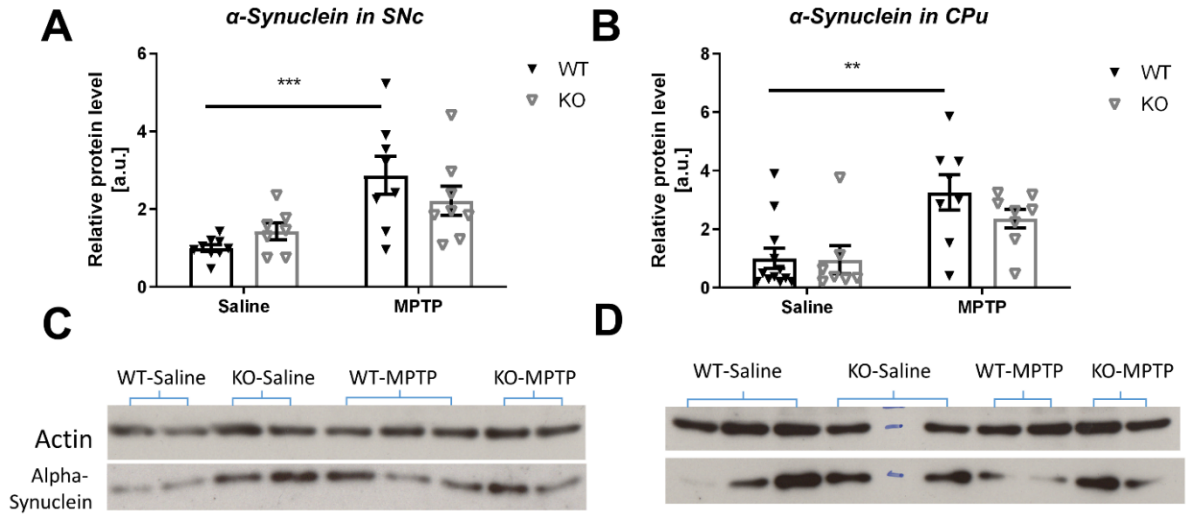

Figure 5-5 Relative protein expression showed a significant increase of aSYN in SNc and CPu

Densitometric quantification of aSYN, measured in SNc (A) and CPu (B) brain samples from WT (black bars) and $Ca_v1.3$ KO mice (grey bars), treated with either saline or MPTP, using immunoblotting. Representative immunoblots for genotype and treatment effects are shown in (C)

for SNc and in (D) for CPu brain regions. ***: $p < 0.001$ and **: $p < 0.01$ for treatment effect of MPTP-treated vs. saline treated WT mice. All values were shown as group mean ±S.E.M.

(A) ANOVA MPTP $p < 0.001$, genotype n.s., MPTP x genotype n.s. (B) ANOVA MPTP $p < 0.001$, genotype n.s., MPTP x genotype n.s. Bonferroni post-test was conducted within the same genotype (*** $p<0.001$, ** $p<0.01$ vs. saline-treated mice).

5.3.2 Relative protein expression of TH

The relative levels of TH protein for all experimental groups are shown in Figure 5-6 for midbrain (SNc) and striatal (CPu) samples. Chronic MPTP treatment induced a significant reduction of TH protein in the midbrain of all mice (MPTP effect: $F_{1,28}$ 7.48, $p<0.01$). By contrast, TH protein levels in striatal tissue samples remained unaffected by chronic MPTP treatment. The Western blot resulted in a single band with the size of 60 kDa, specific to TH.

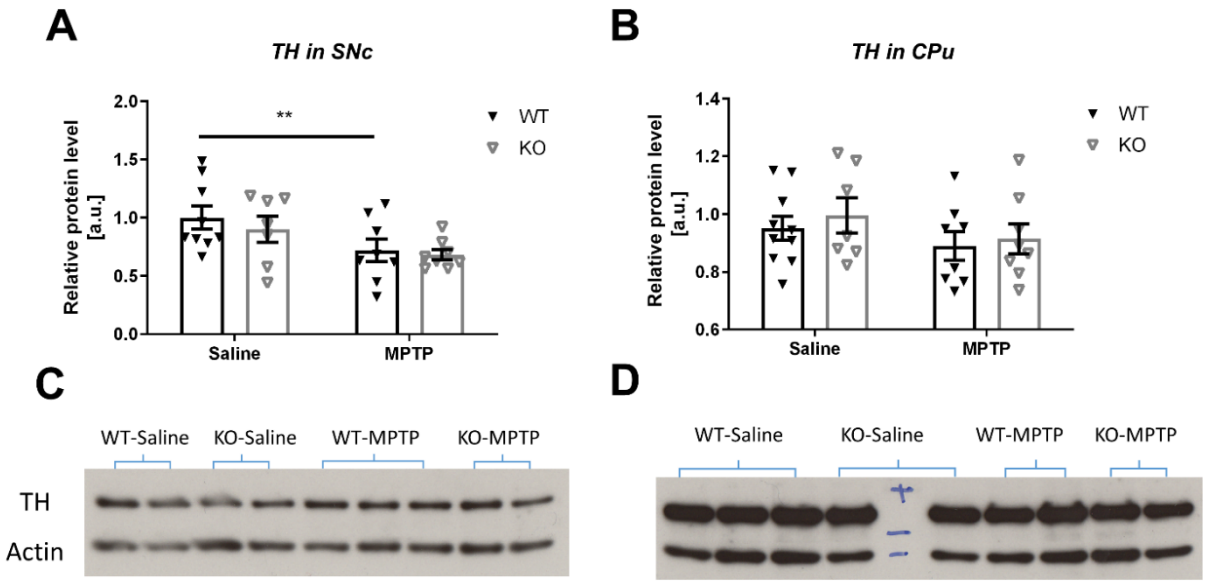

Figure 5-6 Relative protein expression of TH decreased in SNc following MPTP treatment but not in CPu

Densitometric quantification of TH, measured in SNc (A) and CPu (B) brain samples from WT (black bars) and $Ca_v1.3$ KO mice (grey bars), treated with either saline or MPTP, using immunoblotting. Representative immunoblots for genotype and treatment effects are shown in (C) for SNc and in (D) for CPu brain regions. All values are shown as group mean and S.E.M.

(A) ANOVA MPTP $p < 0.01$, genotype n.s., MPTP x genotype n.s. (B) ANOVA MPTP n.s., genotype ns, MPTP x genotype n.s.

5.3.3 Relative protein expression of DAT

Relative protein expressions of DAT in WT saline-treated mice, KO saline-treated mice, WT MPTP-treated mice and KO MPTP-treated mice groups in CPu are shown in Figure 5-7. The Western blot resulted in a single band with the size of 80 kDa for DAT protein. The optical densities of the bands were measured via densitometry and normalized to β-Actin. There was a treatment effect of MPTP in both genotypes (ANOVA, $p < 0.001$), but also an interaction effect, as seen by 2-way ANOVA ($p < 0.05$) and the expressions of DAT in MPTP-treated mice was lower than those in saline-treated $Ca_v1.3$ KO mice.

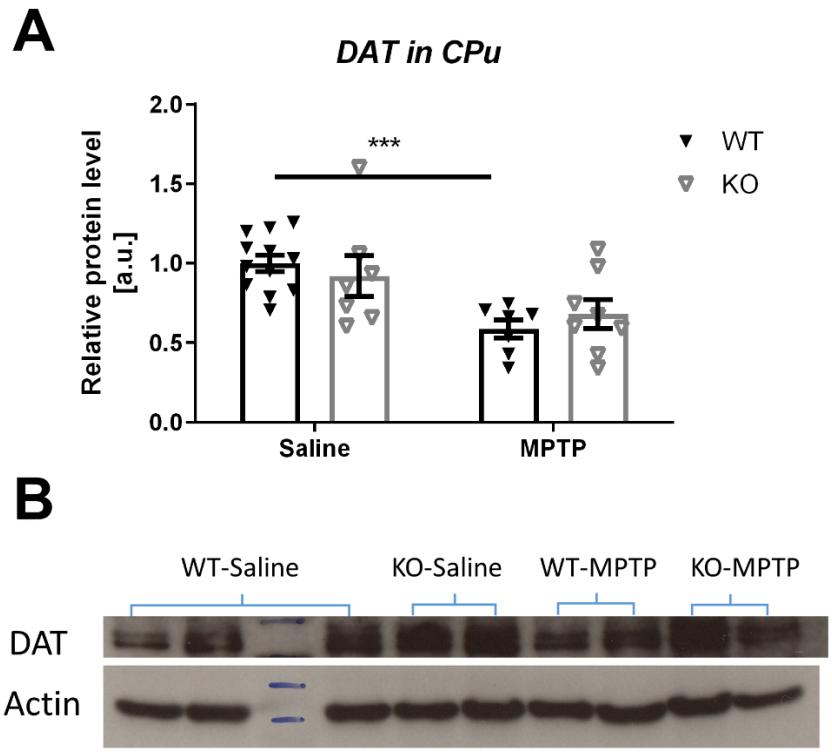

Figure 5-7 Relative protein expression of DAT showed a decrease of DAT after MPTP treatment in CPu, but the extent of DAT depletion in MPTP-treated $Ca_v1.3$ KO mice was not statistically different when compared to WT mice

Densitometric quantification of DAT, measured in CPu (A) brain samples from WT (black bars) and $Ca_v1.3$ KO mice (grey bars), treated with either saline or MPTP using immunoblotting. ***: $p < 0.001$ for treatment effect of MPTP-treated vs. saline treated WT mice. All values are shown as group mean and S.E.M. (A) ANOVA MPTP $p < 0.001$, genotype n.s., MPTP x genotype n.s.

6 Discussion

The vulnerability of the nigro-striatal DA system against MPTP toxicity in mice with $Ca_V1.3$ channel deficiency has so far not been described in detail. This is the first *in vivo* study using a multimodal experimental design to investigate the effects of the mitochondrial toxin MPTP on the integrity of the nigro-striatal DA system in such a mouse model.

6.1 The effect of chronic MPTP treatment on striatal dopamine levels in $Ca_V1.3$ KO mice

In our study chronic MPTP treatment resulted in an overall reduction of striatal DA in mice irrespective of their genotypes. However, in transgenic mice the loss of striatal DA of ~50 % was less pronounced when compared to that of wild-type controls (~70 %), resulting in a relative neuroprotective effect on residual DA levels of ~66 %. For the first time we could demonstrate that genetic "silencing" of $Ca_V1.3$ channels in mice mitigates the toxic actions of chronic MPTP exposure at the functional level as assessed by striatal DA measurement. This is in accordance with a recent pharmacological study showing a preservation of striatal DA in MPTP-treated mice undergoing co-treatment with isradipine, a calcium channel blocker with sufficient affinity to the $Ca_V1.3$ subtype (Wang et al., 2017).

However, former pharmacological animal studies using the MPTP model of PD could not confirm such neuroprotective effects when subjected to the non-selective dihydropyridine antagonist nimodipine (Kupsch et al., 1995; Kupsch et al., 1996), suggesting a different impact of both non-selective $Ca_V1.2/1.3$-channel antagonists on this issue. Referring to the nigral level, an attenuation of DA-ergic cell loss of ~50% in a small group of MPTP-treated mice with $Ca_V1.3$ channel deficiency (n=3) which was analogous to pharmacological "silencing" of $Ca_V1.3$ channels was cursorily reported (Chan et al., 2007). These findings were confirmed in a subsequent preclinical study with 6-hydroxy dopamine (6-OHDA) lesioned mice (Ilijic et al., 2011). From the results of our study it is therefore reasonable to conclude that genetic "silencing" of $Ca_V1.3$ channels may exert neuroprotective effects on the integrity of the nigro-striatal DA system not only at the cellular (Chan et al., 2007) but also at the neurochemical level. This becomes more evident when considering our data on DA turnover. Referring to the MPTP condition, an increased metabolite to DA ratio suggests that more DA is released from surviving nigro-striatal terminals and utilized reflecting a common compensatory mechanism observed not only in PD patients but also in MPTP-treated mice (Rabey and Burns, 2002). In our study a significantly increased DA turnover has only been shown for MPTP-treated wild-type mice, suggesting that the preserved striatal DA-ergic neurotransmission in $Ca_V1.3$ KO mice was so effectual as to hamper the induction of

compensatory mechanisms at the level of DA turnover. Furthermore, the degree of DA turnover in MPTP-treated transgenic mice was in the same range to that seen in all saline-treated controls, suggesting the compensatory increased DA turnover will depend on the extent of striatal DA depletion. The rationale for this assumption derives from *post-mortem* studies in PD patients whose motor symptoms only become apparent when ~80% of striatal DA is lost (Bernheimer et al., 1973), as it has been shown for our chronically MPTP-treated wild-type mice (~70% of DA depletion).

6.2 The effect of chronic MPTP treatment on dopamine synthesis and uptake in $Ca_V1.3$ KO mice

6.2.1 Tyrosine hydroxylase (TH)

Dopamine (DA) is synthesised in catecholaminergic neurons by an enzymatic conversion of tyrosine to levodopa (L-dopa) which is subsequently converted to DA (by the enzyme aromatic acid decarboxylase, AADC). However, the rate-limiting step of DA synthesis is mediated by tyrosine hydroxylase (TH) using tyrosine as substrate. Within the nigro-striatal DA system, the TH protein biosynthesis occurs in cell bodies of neurons of the substantia nigra compacta (SNc) for which reason in preclinical studies nigral TH protein expression (either assessed by immunostaining or Western blot) is often used as a surrogate marker for nigral cell survival and the functioning of the nigro-striatal DA system. In the present study we could demonstrate an overall reduction of midbrain TH protein expression (assessed by Western blot analysis) in all mice undergoing MPTP treatment as a significant treatment effect irrespective of the genotypes. This treatment effect might be indicative of a presumed MPTP-induced neurodegeneration of midbrain DA neurons (including those in the SNc) due to the chronic MPTP treatment. Considering this, particularly for wild-type mice our results are in agreement with previous studies using TH immunostaining (i.e. TH-immunoreactivity [TH-ir]) as a surrogate marker for nigral cell survival showing a nigral cell loss of 23% to 45% following chronic MPTP treatment (Gibrat et al., 2009). However, transferring these TH immunohistochemical data to those of Western blot analysis as obtained in our study, one could expect a MPTP-induced extent of nigral cell death of ~25% in WT mice, although the assessment by Western blot does not necessarily reflect the situation at the morphological level. This issue has recently been investigated in an acute MPTP mouse model showing a discrepancy of TH protein expression in the SNc as a whole vs. cell counts of TH-positive nigral neurons (Kozina et al., 2014). In their study the authors could demonstrate that TH protein expression in the SNc remained unchanged (or was even increased by 29% in

individual nigral cell bodies) while DA-ergic cell loss was estimated to be ~43% which has been discussed as an enhanced DA synthesis due to an increase of TH protein (Kozina et al., 2014). By contrast, in a more recent study a concordant decrease of TH expression of ~50% as assessed by Western blot and TH-ir has been demonstrated (Mariucci et al., 2018). In the present study, the preservation of striatal tissue levels of DA in MPTP-treated mice with a genetic deletion of $Ca_V1.3$ channels was surprisingly not paralleled by a rescue of TH protein expression in midbrain samples but was similar to those seen in wild-type mice. However, the lack of a compensatory increased DA turnover in MPTP-treated $Ca_V1.3$ -/- mice argues against a missing neuroprotection of $Ca_V1.3$ channel deficiency to MPTP toxicity. In fact, our data and the results of previous studies suggest that nigral TH protein expression as assessed by Western blot analysis is not a reliable surrogate marker for the functioning of the nigro-striatal DA system in MPTP mouse models due to its broad variety (Kozina et al., 2014; Mariucci et al., 2018). It is also conceivable that posttranslational modifications of the TH protein may also account for this observation (Jakowec et al., 2004).

This becomes more evident when considering the expression of midbrain TH gene transcripts of chronically MPTP-treated mice. In our study we could show for WT animals a decrease of TH mRNA as assessed by qPCR by means of a significant treatment effect. This observation is in line with previous preclinical studies using *in situ* hybridization analysis (D'Astous et al., 2003; Jakowec et al., 2004; Kuhn et al., 2003) or qPCR technique (Kozina et al., 2017; Xu et al., 2005), respectively. A decrease of TH mRNA has also been reported in PD patients and has (together with the decrease of TH protein) been considered to be enunciative for the severity of the disease progression (Javoy-Agid et al., 1990; Kastner et al., 1993). In the present study, the decrease of TH protein was paralleled with a decline of TH mRNA transcripts, suggesting the lack of a compensatory up-regulation of TH gene expression following chronic MPTP treatment. Thus, our data indicate that MPTP targets both the protein and the gene expression of TH, as suggested elsewhere (Xu et al., 2005). Considering the nigral TH gene expression in MPTP-treated mice with $Ca_v1.3$ channel deficiency, one might conclude a similar effect. However, the decrease of TH mRNA in transgenic $Ca_v1.3$ -/- mice was less pronounced when compared to their MPTP-treated WT littermates. Importantly, we could further show that following chronic MPTP treatment the various genotypes exerted a different response on TH mRNA expression by means of a significant interaction effect. From this point of view, it is interesting to note that in saline-treated transgenic mice (i.e., animals of the control group) the TH mRNA expression *per se* was diminished in comparison to wild-type animals, which was thus far unknown. One explanation for this observation could be that changes in calcium levels may affect gene expression by activating or

inhibiting transcription factors that regulate the expression TH. However, since the striatal TH protein expression in those animals was similar for both genotypes, one cannot conclude a negative feedback mechanism of the protein and thus a regulatory effect on TH gene expression in $Ca_V1.3$ channel deficient mice. The finding of reduced TH mRNA expression and physiological DA content in saline treated $Ca_V1.3$ KO mice suggests some compensatory adaptations. Alternatively, the diminished TH mRNA expression in transgenic $Ca_V1.3$ -/- mice is attributed to a direct effect of the genetic knock out of $Ca_V1.3$ channels by an unknown reason and thus requires further elucidation.

Taken together our results demonstrate that in chronically MPTP-treated $Ca_V1.3$ -/- mice the relative preservation of the nigro-striatal dopamine neurotransmitter system (by means of a neuroprotective effect in response to a genetic silencing of $Ca_v1.3$ channels) was not paralleled by a significant attenuation of midbrain and striatal TH protein expression as assessed by Western blot analysis. By contrast, the expression of TH mRNA remained unchanged. Since MPTP toxicity targets both TH mRNA and protein expression (Xu et al., 2005) our data suggest a compensatory effect on the TH gene regulation and subsequent DA synthesis. However, to better understand these observations, it would be important to provide stereological counts for nigral TH/Nissl neurons which should be elucidated in further studies.

6.2.2 Dopamine transporter (DAT)

In the present study another surrogate marker for investigating DA homeostasis in response to MPTP toxicity was the assessment of dopamine transporter (DAT) protein in striatal tissue samples by Western blot analysis. Due to its implementation in DA re-uptake, in nigro-striatal projection neurons DAT is predominantly located at the pre-synaptic site and thus is often used as a marker for the integrity of the axonal terminals of those neurons. Moreover, DAT may be regarded as the immediate relay station of DA-ergic neurons by which the toxic actions of MPTP are initiated due to the high affinity of its active metabolite MPP^+ (Blandini and Armentero, 2012; Dauer and Przedborski, 2003; Javitch et al., 1985). In line with this, it has been demonstrated that in PD patients (Bernheimer et al., 1973) as well as in MPTP models of PD (Cochiolo et al., 2000; Herkenham et al., 1991) the loss of nerve terminals in the striatum precedes the loss of DA-ergic neurons in the SNc. This suggests that the striatal nerve terminals are the primary site of the MPTP-induced degenerative process. In the present study we could demonstrate an overall reduction of striatal DAT protein expression in all mice undergoing MPTP treatment, suggesting a neurotoxin-induced impairment of the integrity of the axonal terminal of DA-ergic projection neurons

(Muroyama et al., 2011). However, this significant treatment effect was visually more pronounced in wild-type mice which is in agreement with previous studies using *in-vivo* (Jakowec et al., 2004; Kou and Bloomquist, 2007; Lohr et al., 2016) and *ex-vivo* techniques (Muroyama et al., 2011). For instance, in their acute MPTP mouse models *Lohr* and colleagues reported a depletion of striatal DAT expression of ~ 77%, (Lohr et al., 2016). By contrast, *Jakowec* et al. could show less reduction of DAT protein to ~30 to 40% seven days post-lesioning with a subsequent increase to 44 % ± 6 %, 62 % ± 7 %, and 78 % ± 13 % at one, two, and three months after sacrifice, respectively (Jakowec et al., 2004). The latter maybe due to a time-dependent recovery effect in surviving DA neurons (Bezard et al., 2000). On the other hand, a decrease of DAT protein could also be observed in DA-ergic synaptosomes (which were isolated from striatal tissue) on the same order of magnitude (i.e. to ~40 %) even 16 h after an acute MPTP exposure of C57BL/6N mice (Muroyama et al., 2011).

Remarkably, in the present study the extent of depletion of striatal DAT protein in MPTP-treated transgenic $Ca_V1.3$ -/- mice was not statistically different when compared to WT animals, suggesting that the integrity of the axonal terminal field in mice with $Ca_V1.3$ channel deficiency has failed to show a better resistance to chronic MPTP toxicity. On the other hand, the preservation of striatal dopamine in our MPTP $Ca_V1.3$ cohort does not reflect a breakdown of nigro-striatal synapses in the same order of magnitude in WT animals subjected to MPTP. Alternatively, this observation could instead be due to a methodological issue rather than it being an argument against our hypothesis, whereby the genetic silencing of $Ca_V1.3$ channels might attenuate the toxic effects of MPTP by means of neuroprotection. Thus, in our experiments for DAT protein analysis in striatal tissue samples, the dorsolateral portion of the caudate putamen was omitted since punches of this region were previously taken for HPLC-based neurotransmitter assessment. Considering the facts that (i) the majority of nigro-striatal projections terminates in the dorsolateral portion of the caudate putamen (Haber, 2014, 2016) and (ii) only 10 to 15 % of the nerve terminals are DA-ergic (Mallajosyula et al., 2008), one could argue that our results for DAT were not representative for the entire striatum. On the other hand, these results are partly in line with previous observations of our lab. Thus, in transgenic $Ca_V1.3$ -/- mice subjected to an acute MPTP paradigm, a significant reduction of striatal TH fibre density could be observed which was visually less pronounced compared to WT animals. In these experiments densitometric measurement of striatal TH-ir fibre density was used as a comparative technique for investigating the integrity of axonal terminals of nigro-striatal projection neurons (own observation).

However, considering the genetic transcripts of DAT, we could show a significant preservation of DAT mRNA in midbrain samples of $Ca_V1.3$ -/- mice as assessed by qPCR analysis. Thus, chronic MPTP treatment resulted in a significant reduction of midbrain DAT mRNA only in WT animals, which is in good agreement with previous studies using *in-situ* hybridisation technique (Kuhn et al., 2003) or qPCR analysis (Xu et al., 2005) in mice subjected to an acute MPTP paradigm. The reduction of DAT mRNA in midbrain samples of chronically MPTP-treated WT mice may reflect a direct targeting of the neurotoxin at the DNA level as already discussed for nigral TH gene expression (see above, cf. (Xu et al., 2005). In other words, the MPTP-induced reduction in nigral DAT mRNA is the consequence of DA-ergic neuron death in WT mice. In this regard, it is important to note that MPTP did not exert any alteration of the DAT gene in transgenic mice with $Ca_V1.3$ channel deficiency, indicating their lesser vulnerability to MPTP toxicity. Further studies are needed to provide stereological cell counts for nigral TH-ir/Nissl neurons for a better understanding.

Alternatively, a compensatory regulation of the DAT gene in response to the nigral DAT protein level may also account for the observed effects. However, although no data on midbrain DAT protein expression were available (due to the experimental design of our study), such a mechanism seems very unlikely. For example, if reduced DAT mRNA were the result of down regulating gene expression, one might assume a concomitant increase of DAT protein under the condition of MPTP toxicity, which kills nigral neurons. *Vice versa,* a compensatory decrease of DAT protein in transgenic $Ca_V1.3$ -/- mice because of DAT mRNA up regulation cannot be concluded from the results of our other surrogate markers investigated (e.g. TH expression and DA-ergic neurotransmission).

Previous data suggest that DA-ergic terminals are the primary site of the degenerative process, and the neuronal death in PD as well as under the MPTP condition may result from a dying back process of nigro-striatal projection neurons (Bernheimer et al., 1973; Cochiolo et al., 2000; Herkenham et al., 1991). Moreover, it could be clarified that the molecular pathways underlying destruction of the cell soma are separate and distinct from those which mediate destruction of axons (Raff et al., 2002). With regard to our study, it is therefore conceivable that the lesser decrease in DAT protein level in the striatum of $Ca_V1.3$-channel deficient mice and the concomitant significant increase of nigral DAT mRNA may reflect an interrupted axonal transport of the DAT protein due to the dying back mechanism induced by MPTP.

6.3 The effect of chronic MPTP treatment on the expression of alpha-synuclein in $Ca_V1.3$ KO mice

There was no difference in alpha-synuclein (aSYN) at the protein level between wild-type and $Ca_V1.3$-/- mice after saline treatment in either SNc or CPU samples, suggesting that under normal conditions the $Ca_V1.3$ channel deficiency does not alter the aSYN protein expression.

Examination of the change of aSYN protein expression induced by MPTP treatment found aSYN to be significantly increased in midbrain extracts of WT mice treated with chronic intoxication by about ~190%. The finding matches the results of another study which also showed progressively increased aSYN protein level in midbrain extracts 0 to 4 days after chronic MPTP administration (Vila et al., 2000). In their study, after the chronic MPTP regimen aSYN protein expression progressively increased in midbrain extracts from day 0 (+44%) to day 4 days at peak (77%) and then returned to control level at day 7. While our results showed 190% increase of aSYN after 4.5 weeks, the different pattern of aSYN alteration can be explained by cumulative dosage of MPTP (our study: 190 mg/kg vs. Vila's study: 150 mg/kg) and injection period of MPTP (our study: 4.5 weeks vs one week). When mice were treated with chronic administration, the dopaminergic neurons were killed mostly by apoptosis rather than necrosis (Jackson-Lewis et al., 1995; Tatton and Kish, 1997). The comparatively long-term administration is more likely to increase aSYN protein expression for a longer period than that of intensive injections. And it raises the possibility that this pattern may cause neuron apoptosis more thoroughly. This can be supported by the fact that the number of aSYN positive neurons was still increased by day 7 and only appeared to return to baseline after day 14 (Vila et al., 2000).

In the present study, we could also demonstrate a significant increase of aSYN in the striatum. However, this observation does not match the findings from the *Vila*s study in which no changes in aSYN protein expression were reported. Indeed, aSYN immunostaining was also observed at the striatal level, thus in the terminal field of nigro-striatal projection neurons. A possible explanation for the discrepancy is that it is due to the slight differences in method settings, for example the animal age and MPTP treatment (Tatton and Kish, 1997).

However, in our study aSYN protein expression was increased in striatal and nigral brain samples in all mice undergoing chronic MPTP treatment, i.e. irrespective of their genotype suggesting that aSYN expression was independent on calcium under the condition of mitochondrial dysfunction induced by MPTP. It has been proposed that a multifactorial relationship of aSYN with calcium

signaling where elevations in intracellular calcium can result in the aggregation and release of aSYN or *vice versa* accounts for the neurodegenerative process within the nigro-striatal DA system (for review see Leandrou et al., 2019). Since the expression of aSYN following chronic MPTP treatment has been described earlier and could be even addressed to *Lewy*-body-like pathology (Meredith et al., 2002), one might argue that aSYN expression and aggregation is rather related to mitochondrial dysfunction alone. Currently there is no direct evidence that presynaptic calcium channels (i.e., VGCC) regulate aSYN propagation. On the other hand, from the results of our study we cannot conclude the formation of misfolded aggregates of aSYN since only total aSYN (including monomeric, oligomeric and fibril forms) was assessed by Western blot analysis.

In contrast to the increased expression of aSYN protein following MPTP, the genetic transcripts of aSYN remained unchanged as assessed by qPCR. Considering the similar orders of magnitude in the expression rates of aSYN in all brain samples, post-translational modifications of the protein in our model may be suggested. This might result from different forms of aSYN. Physiologically, aSYN remains in its monomeric form, while under pathological conditions (like chronic MPTP treatment) the formation of misfolded aggregates or even fibrils occur. These post-translational modifications may have no effect on aSYN mRNA expression via negative transcriptional feedback. On the other hand, several studies have investigated the mRNA expression in post-mortem brain samples of sporadic PD patients and showed controversial results. Increased vs. not-altered vs. decreased aSYN mRNA expression in SNc have been reported by different study groups, summarized by (Kim and Lee, 2008). In the same manner, in different MPTP mouse models of PD, contradictory results have also been reported (Kuhn et al., 2003; Meredith et al., 2002; Vila et al., 2000). For example, in *Kuhn*'s study, there was no sign of changes in mRNA expression after sub-chronic MPTP treatment, which is similar to our MPTP chronic treatment protocol, while the acute MPTP-treated mice showed up-regulated gene expression along with the cell loss (Kuhn et al., 2003). One plausible reason for the "no change" pattern is that the induced protein over-expression conversely inhibits the mRNA synthesis during a comparatively long period of treatment. However, this result is in contrast to the findings that the aSYN mRNA expression was increased in midbrain consistent with aSYN protein alterations in a time-dependent manner, peaking at 4 days after intoxication and then returning to the normal level by 21 days (Vila et al., 2000). In another study conducted by *Meredith* et al. it was shown that the mRNA expression of aSYN was significantly decreased at 1 and 3 weeks after treatment, but it returned to the same level as control groups at 24 weeks (Meredith et al., 2002). It is worth discussing the discrepancy among these studies. Firstly, although the three studies used different methods to

measure the mRNA comparative quantities in brain tissues, these RNA measurements were sophisticated in bioresearch. Therefore, there is no doubt that the different methods would affect the results. Secondly, although we used so-called “chronic MPTP treatment”, the processes of MPTP administration and animal conditions are not exactly the same. When mice were treated with MPTP chronically, DA neuron loss could be detected, and it is believed that the apoptosis plays a key role in cell death rather than the necrosis caused by acute treatment. And this difference may change the expression of mRNA in those regions.

Therefore, one should be cautious when applying aSYN mRNA expression as a biomarker for the progression and severity of PD.

6.4 Study limitations

6.4.1 The modified chronic MPTP model

For the present study, a chronic dosage regime of MPTP was adapted to the protocol of (Luchtman et al., 2009). The modifications comprised (i) the total number of MPTP injections (9 vs. 10) and (ii) the absence of the co-drug probenecid. Probenecid (P) was first shown to inhibit the excretion of urine and urinary MPTP N-oxide shortly after MPTP administration, which may increase the neurotoxic action of MPTP in mice (Lau et al., 1990). Over the past few years the MPTP/P PD animal model was used widely because it could potentiate the toxic effects of MPTP. However, in this study we used the aforementioned modifications since we observed an increased mortality rate in our MPTP cohort when using the original paradigm.

6.4.2 Detection of different aSYN species

The pre-synaptic protein aSYN has been considered to play a key role in the development of PD. There are different structural forms of this protein: monomer, oligomer and fibril. It is worth discussing which of these forms is neurotoxic. aSYN itself is non-toxic and commonly distributed: not only in CNS but also in red blood cells (Nakai et al., 2007). On the other hand, fibrillary aSYN is the main component of *Lewy* bodies, which are the pathological hallmark of Parkinson’s disease. *Lewy* bodies are final products rather than toxic, because: (i) *Lewy* bodies have been identified in 8-17% of neurologically normal individuals over 60, according to a post-mortem study (Frigerio et al., 2011), (ii) *Lewy* body formation is absent in patients with familial mutations in the *PARKIN* gene or *LRRK2* gene (Cookson et al., 2008; Gaig et al., 2007). Together with these factors, oligomers of aSYN and the biological effects of different oligomers have drawn great attention. Danzer et al found that some types of oligomers could trigger cell death, while others are able to

enter cells directly and seed intracellular aSYN aggregation in an *in-vitro* study (Danzer et al., 2007). Postmortem studies in PD patients and *in-vivo* studies also indicate that aSYN oligomers are toxic (Periquet et al., 2007; Sharon et al., 2003).

Although aSYN oligomers are a research hotspot and they are suspected to be toxic, the exact role of oligomers in pathological development of PD still remains unclear because the vast majority of studies have used *in-vitro* formed oligomers, and until now aSYN oligomers have not been detected *in-situ* (Bengoa-Vergniory et al., 2017). Besides, there is no such perfect antibody which can be used to specifically recognize one particular type of aSYN species (Kumar et al., 2020). In their study they tested antibodies which were previously claimed to be specific to oligomers, but found out that all of them could recognize not only oligomers but also aSYN fibrils. Based on aforementioned factors and laboratory conditions, we detected total aSYN protein with urea sample buffer and did not perform a specific aSYN oligomer experiment.

6.4.3 Quantification of TH neurons in SNc

The estimated number of survival neurons can be analysed by counting TH-immunoreactive cell bodies. However, in this study, immunohistochemistry was not done because all tissue processing steps were done in naïve brains (i.e. in non-fixated tissue). Further studies are mandatory to investigate this issue.

6.5 Clinical implications and conclusions

The present study provides further *in-vivo* evidence for the interplay of calcium and mitochondrial dysfunction (induced by MPTP) in the breakdown of the nigro-striatal DA system. Although a cure for Parkinson's disease has yet to be found, many scientists are still searching for neuroprotective strategies. Numerous molecules have been evaluated in terms of neuroprotection in preclinical settings (*in-vitro* and *in-vivo*) and $Ca_V1.3$ channels are potential therapeutical targets for neuroprotection of PD. Over the past years, several pre-clinical studies have investigated the potential protective effects of DHPs and $Ca_V1.3^{-/-}$ mice in models of PD, with many showing promising results. In 8 of the 13 reports, a significant neuroprotection effect was reported for the brain-permeable DHPs isradipine, nimodipine, and nifedipine (Liss and Striessnig, 2019). However, the experimental design of these studies varied, including the PD model used (6-OHDA vs. MPTP), animals (species, strain, age, and sex), treatment regimen (DHP, treatment onset, route of administration, and dosing interval), readout (approach and methodology), and plasma concentrations. These differences made it difficult to draw an overall conclusion. Therefore, using a standardized approach in future studies could help to better interpret and compare the obtained

results. Here, it is also noteworthy that a study failed to show evidence for neuroprotection in $Ca_V1.3^{-/-}$ mice, which showed contrary results from ours (Ortner et al., 2017). A compensatory mechanism may account for this difference: $Ca_V1.3$ knockout may lead to compensatory changes in Ca^{2+} channel expression during development, replacing a role of $Ca_V1.3$ channels (Poetschke et al., 2015). It is also possible that inconsistent results are due to differences in experimental design, as in our study MPTP was administrated and they used 6-OHDA. Overall, the voltage-gated Ca^{2+} channels still represent an attractive drug target for the therapy of PD (Ortner, 2021).

It is not surprising that, the phase 3 STEADY-PD III clinical trial with the isradipine as treatment in early PD patients failed to reach its primary endpoint. There are several reasons that could explain the failure. Firstly, the role of calcium channel compensation: the expression of calcium channels, either Cav1 channel or other calcium channels with similar functions, can be upregulated in SNc DA neurons *in-vivo* if the calcium channels are blocked by isradipine (Guzman et al., 2018). For example, significant higher mRNA-levels of $Ca_V3.1$ in SNc DA neurons were found in $Ca_V1.3$ KO mice when compared to WT mice, and cytosolic Ca^{2+} oscillations remained almost unchanged (Poetschke et al., 2015). Secondly, the issue of systemic drug administration: even if PD is caused by mitochondrial damage via Ca^{2+} entry through Ca_V1 channels, it is possible that 5 mg isradipine twice a day is insufficient for engaging the target calcium channels (Ortner et al., 2017; Parkinson Study Group, 2020). There was also a high dosage group (10 mg twice daily) in the phase II study and a suggestion of a trend toward increasing benefit at higher dosages was found (Parkinson Study, 2013). However, higher dosages could cause some unwanted or serious side effects (e.g., headache, dizziness and syncope), and it is not recommended for PD patients. Thirdly, "early stage" is not early: In terms of the "early stage", the progression of PD is slow and gradual. Usually by the time PD is diagnosed, the pathology is likely to be widespread (Halliday et al., 2011). Thus, it seems unreasonable to rely on normal dose CCB to rescue the neurons from aSYN aggregation and cell death for various reasons. Besides the low selectivity of isradipine for $Ca_V1.3$ channels (Ortner et al., 2017), the ongoing aSYN pathology may explain the lack of neuroprotection in early-stage PD patients treated with isradipine (Biglan et al., 2017; Parkinson Study Group, 2020). Indeed, underlying PD symptoms there is a complex pathological mechanism which leads to SNc DA cell death, and most of the studies have only focused on one pathophysiology using toxin animal models. Therefore, further studies are needed to better understand the interplay of pathogenetic mechanism(s) of PD. Besides, combination of the tested neuroprotective agents ('cocktail') which has been hypothesized by some scientists could be effective (Salamon et al.,

2020), and we hope that in the near future neuroprotective cocktails with highly selective calcium channel blockers will find their way into PD clinical trials.

7 References

Bengoa-Vergniory, N., Roberts, R.F., Wade-Martins, R., and Alegre-Abarrategui, J. (2017). Alpha-synuclein oligomers: a new hope. Acta Neuropathol *134*, 819-838.

Bernheimer, H., Birkmayer, W., Hornykiewicz, O., Jellinger, K., and Seitelberger, F. (1973). Brain dopamine and the syndromes of Parkinson and Huntington. Clinical, morphological and neurochemical correlations. J Neurol Sci *20*, 415-455.

Betzer, C., Lassen, L.B., Olsen, A., Kofoed, R.H., Reimer, L., Gregersen, E., Zheng, J., Cali, T., Gai, W.P., Chen, T.*, et al.* (2018). Alpha-synuclein aggregates activate calcium pump SERCA leading to calcium dysregulation. EMBO Rep *19*.

Bezard, E., Dovero, S., Imbert, C., Boraud, T., and Gross, C.E. (2000). Spontaneous long-term compensatory dopaminergic sprouting in MPTP-treated mice. Synapse *38*, 363-368.

Biglan, K.M., Oakes, D., Lang, A.E., Hauser, R.A., Hodgeman, K., Greco, B., Lowell, J., Rockhill, R., Shoulson, I., Venuto, C.*, et al.* (2017). A novel design of a Phase III trial of isradipine in early Parkinson disease (STEADY-PD III). Ann Clin Transl Neurol *4*, 360-368.

Blandini, F., and Armentero, M.T. (2012). Animal models of Parkinson's disease. FEBS J *279*, 1156-1166.

Boumezbeur, F., Mason, G.F., de Graaf, R.A., Behar, K.L., Cline, G.W., Shulman, G.I., Rothman, D.L., and Petersen, K.F. (2010). Altered brain mitochondrial metabolism in healthy aging as assessed by in vivo magnetic resonance spectroscopy. J Cereb Blood Flow Metab *30*, 211-221.

Calabresi, P., Mechelli, A., Natale, G., Volpicelli-Daley, L., Di Lazzaro, G., and Ghiglieri, V. (2023). Alpha-synuclein in Parkinson's disease and other synucleinopathies: from overt neurodegeneration back to early synaptic dysfunction. Cell Death Dis *14*, 176.

Callio, J., Oury, T.D., and Chu, C.T. (2005). Manganese superoxide dismutase protects against 6-hydroxydopamine injury in mouse brains. J Biol Chem *280*, 18536-18542.

Cannon, J.R., and Greenamyre, J.T. (2011). The role of environmental exposures in neurodegeneration and neurodegenerative diseases. Toxicol Sci *124*, 225-250.

Catterall, W.A., Perez-Reyes, E., Snutch, T.P., and Striessnig, J. (2005). International Union of Pharmacology. XLVIII. Nomenclature and structure-function relationships of voltage-gated calcium channels. Pharmacol Rev *57*, 411-425.

Chan, C.S., Guzman, J.N., Ilijic, E., Mercer, J.N., Rick, C., Tkatch, T., Meredith, G.E., and Surmeier, D.J. (2007). 'Rejuvenation' protects neurons in mouse models of Parkinson's disease. Nature *447*, 1081-1086.

Chia, S.J., Tan, E.K., and Chao, Y.X. (2020). Historical Perspective: Models of Parkinson's Disease. Int J Mol Sci *21*.

Chinta, S.J., and Andersen, J.K. (2005). Dopaminergic neurons. Int J Biochem Cell Biol *37*, 942-946.

Clark, N.C., Nagano, N., Kuenzi, F.M., Jarolimek, W., Huber, I., Walter, D., Wietzorrek, G., Boyce, S., Kullmann, D.M., Striessnig, J.*, et al.* (2003). Neurological phenotype and synaptic function in mice lacking the CaV1.3 alpha subunit of neuronal L-type voltage-dependent Ca2+ channels. Neuroscience *120*, 435-442.

Cochiolo, J.A., Ehsanian, R., and Bruck, D.K. (2000). Acute ultrastructural effects of MPTP on the nigrostriatal pathway of the C57BL/6 adult mouse: evidence of compensatory plasticity in nigrostriatal neurons. J Neurosci Res *59*, 126-135.

Cookson, M.R., Hardy, J., and Lewis, P.A. (2008). Genetic neuropathology of Parkinson's disease. Int J Clin Exp Pathol *1*, 217-231.

D'Astous, M., Morissette, M., Tanguay, B., Callier, S., and Di Paolo, T. (2003). Dehydroepiandrosterone (DHEA) such as 17beta-estradiol prevents MPTP-induced dopamine depletion in mice. Synapse *47*, 10-14.

Danzer, K.M., Haasen, D., Karow, A.R., Moussaud, S., Habeck, M., Giese, A., Kretzschmar, H., Hengerer, B., and Kostka, M. (2007). Different species of alpha-synuclein oligomers induce calcium influx and seeding. J Neurosci *27*, 9220-9232.

Dauer, W., and Przedborski, S. (2003). Parkinson's disease: mechanisms and models. Neuron *39*, 889-909.

de Lau, L.M., and Breteler, M.M. (2006). Epidemiology of Parkinson's disease. Lancet Neurol *5*, 525-535.

Dias, V., Junn, E., and Mouradian, M.M. (2013). The role of oxidative stress in Parkinson's disease. J Parkinsons Dis *3*, 461-491.

Fahn, S., and Parkinson Study, G. (2005). Does levodopa slow or hasten the rate of progression of Parkinson's disease? J Neurol *252 Suppl 4*, IV37-IV42.

Follett, J., Darlow, B., Wong, M.B., Goodwin, J., and Pountney, D.L. (2013). Potassium depolarization and raised calcium induces alpha-synuclein aggregates. Neurotox Res *23*, 378-392.

Frigerio, R., Fujishiro, H., Ahn, T.B., Josephs, K.A., Maraganore, D.M., DelleDonne, A., Parisi, J.E., Klos, K.J., Boeve, B.F., Dickson, D.W.*, et al.* (2011). Incidental Lewy body disease: do some cases represent a preclinical stage of dementia with Lewy bodies? Neurobiol Aging *32*, 857-863.

Gaig, C., Marti, M.J., Ezquerra, M., Rey, M.J., Cardozo, A., and Tolosa, E. (2007). G2019S LRRK2 mutation causing Parkinson's disease without Lewy bodies. J Neurol Neurosurg Psychiatry *78*, 626-628.

Gandhi, S., Wood-Kaczmar, A., Yao, Z., Plun-Favreau, H., Deas, E., Klupsch, K., Downward, J., Latchman, D.S., Tabrizi, S.J., Wood, N.W.*, et al.* (2009). PINK1-associated Parkinson's disease is caused by neuronal vulnerability to calcium-induced cell death. Mol Cell *33*, 627-638.

George, S., Rey, N.L., Reichenbach, N., Steiner, J.A., and Brundin, P. (2013). alpha-Synuclein: the long distance runner. Brain Pathol *23*, 350-357.

Ghiglieri, V., Calabrese, V., and Calabresi, P. (2018). Alpha-Synuclein: From Early Synaptic Dysfunction to Neurodegeneration. Front Neurol *9*, 295.

Gibrat, C., Saint-Pierre, M., Bousquet, M., Levesque, D., Rouillard, C., and Cicchetti, F. (2009). Differences between subacute and chronic MPTP mice models: investigation of dopaminergic neuronal degeneration and alpha-synuclein inclusions. J Neurochem *109*, 1469-1482.

Gleichmann, M., and Mattson, M.P. (2011). Neuronal calcium homeostasis and dysregulation. Antioxid Redox Signal *14*, 1261-1273.

Gough, D.R., and Cotter, T.G. (2011). Hydrogen peroxide: a Jekyll and Hyde signalling molecule. Cell Death Dis *2*, e213.

Greenamyre, J.T., and Hastings, T.G. (2004). Biomedicine. Parkinson's--divergent causes, convergent mechanisms. Science *304*, 1120-1122.

Grenn, F.P., Kim, J.J., Makarious, M.B., Iwaki, H., Illarionova, A., Brolin, K., Kluss, J.H., Schumacher-Schuh, A.F., Leonard, H., Faghri, F.*, et al.* (2020). The Parkinson's Disease Genome-Wide Association Study Locus Browser. Mov Disord *35*, 2056-2067.

Guzman, J.N., Ilijic, E., Yang, B., Sanchez-Padilla, J., Wokosin, D., Galtieri, D., Kondapalli, J., Schumacker, P.T., and Surmeier, D.J. (2018). Systemic isradipine treatment diminishes calcium-dependent mitochondrial oxidant stress. J Clin Invest *128*, 2266-2280.

Haber, S.N. (2014). The place of dopamine in the cortico-basal ganglia circuit. Neuroscience *282*, 248-257.

Haber, S.N. (2016). Corticostriatal circuitry. Dialogues Clin Neurosci *18*, 7-21.

Halliday, G., Lees, A., and Stern, M. (2011). Milestones in Parkinson's disease--clinical and pathologic features. Mov Disord *26*, 1015-1021.

Halliwell, B. (1992). Reactive oxygen species and the central nervous system. J Neurochem *59*, 1609-1623.

Hasbani, D.M., Perez, F.A., Palmiter, R.D., and O'Malley, K.L. (2005). Dopamine depletion does not protect against acute 1-methyl-4-phenyl-1,2,3,6-tetrahydropyridine toxicity in vivo. J Neurosci *25*, 9428-9433.

Henchcliffe, C., and Beal, M.F. (2008). Mitochondrial biology and oxidative stress in Parkinson disease pathogenesis. Nat Clin Pract Neurol *4*, 600-609.

Herkenham, M., Little, M.D., Bankiewicz, K., Yang, S.C., Markey, S.P., and Johannessen, J.N. (1991). Selective retention of MPP+ within the monoaminergic systems of the primate brain following MPTP administration: an in vivo autoradiographic study. Neuroscience *40*, 133-158.

Hettiarachchi, N.T., Parker, A., Dallas, M.L., Pennington, K., Hung, C.C., Pearson, H.A., Boyle, J.P., Robinson, P., and Peers, C. (2009). alpha-Synuclein modulation of Ca2+ signaling in human neuroblastoma (SH-SY5Y) cells. J Neurochem *111*, 1192-1201.

Hwang, O. (2013). Role of oxidative stress in Parkinson's disease. Exp Neurobiol *22*, 11-17.

Ilijic, E., Guzman, J.N., and Surmeier, D.J. (2011). The L-type channel antagonist isradipine is neuroprotective in a mouse model of Parkinson's disease. Neurobiol Dis *43*, 364-371.

Jackson-Lewis, V., Jakowec, M., Burke, R.E., and Przedborski, S. (1995). Time course and morphology of dopaminergic neuronal death caused by the neurotoxin 1-methyl-4-phenyl-1,2,3,6-tetrahydropyridine. Neurodegeneration *4*, 257-269.

Jackson-Lewis, V., and Przedborski, S. (2007). Protocol for the MPTP mouse model of Parkinson's disease. Nat Protoc *2*, 141-151.

Jakowec, M.W., Nixon, K., Hogg, E., McNeill, T., and Petzinger, G.M. (2004). Tyrosine hydroxylase and dopamine transporter expression following 1-methyl-4-phenyl-1,2,3,6-tetrahydropyridine-induced neurodegeneration of the mouse nigrostriatal pathway. J Neurosci Res *76*, 539-550.

Javitch, J.A., D'Amato, R.J., Strittmatter, S.M., and Snyder, S.H. (1985). Parkinsonism-inducing neurotoxin, N-methyl-4-phenyl-1,2,3,6 -tetrahydropyridine: uptake of the metabolite N-methyl-4-phenylpyridine by dopamine neurons explains selective toxicity. Proc Natl Acad Sci U S A *82*, 2173-2177.

Javoy-Agid, F., Hirsch, E.C., Dumas, S., Duyckaerts, C., Mallet, J., and Agid, Y. (1990). Decreased tyrosine hydroxylase messenger RNA in the surviving dopamine neurons of the substantia nigra in Parkinson's disease: an in situ hybridization study. Neuroscience *38*, 245-253.

Kamel, F., Tanner, C., Umbach, D., Hoppin, J., Alavanja, M., Blair, A., Comyns, K., Goldman, S., Korell, M., Langston, J.*, et al.* (2007). Pesticide exposure and self-reported Parkinson's disease in the agricultural health study. Am J Epidemiol *165*, 364-374.

Kann, O., and Kovacs, R. (2007). Mitochondria and neuronal activity. Am J Physiol Cell Physiol *292*, C641-657.

Kastner, A., Hirsch, E.C., Herrero, M.T., Javoy-Agid, F., and Agid, Y. (1993). Immunocytochemical quantification of tyrosine hydroxylase at a cellular level in the mesencephalon of control subjects and patients with Parkinson's and Alzheimer's disease. J Neurochem *61*, 1024-1034.

Kim, C., and Lee, S.J. (2008). Controlling the mass action of alpha-synuclein in Parkinson's disease. J Neurochem *107*, 303-316.

Kish, S.J., Shannak, K., and Hornykiewicz, O. (1988). Uneven pattern of dopamine loss in the striatum of patients with idiopathic Parkinson's disease. Pathophysiologic and clinical implications. N Engl J Med *318*, 876-880.

Kou, J., and Bloomquist, J.R. (2007). Neurotoxicity in murine striatal dopaminergic pathways following long-term application of low doses of permethrin and MPTP. Toxicol Lett *171*, 154-161.

Kozina, E.A., Khakimova, G.R., Khaindrava, V.G., Kucheryanu, V.G., Vorobyeva, N.E., Krasnov, A.N., Georgieva, S.G., Kerkerian-Le Goff, L., and Ugrumov, M.V. (2014). Tyrosine hydroxylase expression and activity in nigrostriatal dopaminergic neurons of MPTP-treated mice at the presymptomatic and symptomatic stages of parkinsonism. J Neurol Sci *340*, 198-207.

Kozina, E.A., Kim, A.R., Kurina, A.Y., and Ugrumov, M.V. (2017). Cooperative synthesis of dopamine by non-dopaminergic neurons as a compensatory mechanism in the striatum of mice with MPTP-induced Parkinsonism. Neurobiol Dis *98*, 108-121.

Kuhn, K., Wellen, J., Link, N., Maskri, L., Lubbert, H., and Stichel, C.C. (2003). The mouse MPTP model: gene expression changes in dopaminergic neurons. Eur J Neurosci *17*, 1-12.

Kumar, S.T., Jagannath, S., Francois, C., Vanderstichele, H., Stoops, E., and Lashuel, H.A. (2020). How specific are the conformation-specific alpha-synuclein antibodies? Characterization and validation of 16 alpha-synuclein conformation-specific antibodies using well-characterized preparations of alpha-synuclein monomers, fibrils and oligomers with distinct structures and morphology. Neurobiol Dis *146*, 105086.

Kupsch, A., Gerlach, M., Pupeter, S.C., Sautter, J., Dirr, A., Arnold, G., Opitz, W., Przuntek, H., Riederer, P., and Oertel, W.H. (1995). Pretreatment with nimodipine prevents MPTP-induced neurotoxicity at the nigral, but not at the striatal level in mice. Neuroreport *6*, 621-625.

Kupsch, A., Sautter, J., Schwarz, J., Riederer, P., Gerlach, M., and Oertel, W.H. (1996). 1-Methyl-4-phenyl-1,2,3,6-tetrahydropyridine-induced neurotoxicity in non-human primates is antagonized by pretreatment with nimodipine at the nigral, but not at the striatal level. Brain Res *741*, 185-196.

Lang, A.E., Siderowf, A.D., Macklin, E.A., Poewe, W., Brooks, D.J., Fernandez, H.H., Rascol, O., Giladi, N., Stocchi, F., Tanner, C.M.*, et al.* (2022). Trial of Cinpanemab in Early Parkinson's Disease. N Engl J Med *387*, 408-420.

Langston, J.W., Ballard, P., Tetrud, J.W., and Irwin, I. (1983). Chronic Parkinsonism in humans due to a product of meperidine-analog synthesis. Science *219*, 979-980.

Lau, Y.S., Trobough, K.L., Crampton, J.M., and Wilson, J.A. (1990). Effects of probenecid on striatal dopamine depletion in acute and long-term 1-methyl-4-phenyl-1,2,3,6-tetrahydropyridine (MPTP)-treated mice. Gen Pharmacol *21*, 181-187.

Lees, A.J. (2007). Unresolved issues relating to the shaking palsy on the celebration of James Parkinson's 250th birthday. Mov Disord *22 Suppl 17*, S327-334.

Lees, A.J., Hardy, J., and Revesz, T. (2009). Parkinson's disease. Lancet *373*, 2055-2066.

Leong, S.L., Cappai, R., Barnham, K.J., and Pham, C.L. (2009). Modulation of alpha-synuclein aggregation by dopamine: a review. Neurochem Res *34*, 1838-1846.

Licker, V., Turck, N., Kovari, E., Burkhardt, K., Cote, M., Surini-Demiri, M., Lobrinus, J.A., Sanchez, J.C., and Burkhard, P.R. (2014). Proteomic analysis of human substantia nigra identifies novel candidates involved in Parkinson's disease pathogenesis. Proteomics *14*, 784-794.

Liss, B., and Striessnig, J. (2019). The Potential of L-Type Calcium Channels as a Drug Target for Neuroprotective Therapy in Parkinson's Disease. Annu Rev Pharmacol Toxicol *59*, 263-289.

Lohr, K.M., Chen, M., Hoffman, C.A., McDaniel, M.J., Stout, K.A., Dunn, A.R., Wang, M., Bernstein, A.I., and Miller, G.W. (2016). Vesicular Monoamine Transporter 2 (VMAT2) Level Regulates MPTP Vulnerability and Clearance of Excess Dopamine in Mouse Striatal Terminals. Toxicol Sci *153*, 79-88.

Lowe, R., Pountney, D.L., Jensen, P.H., Gai, W.P., and Voelcker, N.H. (2004). Calcium(II) selectively induces alpha-synuclein annular oligomers via interaction with the C-terminal domain. Protein Sci *13*, 3245-3252.

Luchtman, D.W., Shao, D., and Song, C. (2009). Behavior, neurotransmitters and inflammation in three regimens of the MPTP mouse model of Parkinson's disease. Physiol Behav *98*, 130-138.

Ludtmann, M.H.R., Kostic, M., Horne, A., Gandhi, S., Sekler, I., and Abramov, A.Y. (2019). LRRK2 deficiency induced mitochondrial Ca(2+) efflux inhibition can be rescued by Na(+)/Ca(2+)/Li(+) exchanger upregulation. Cell Death Dis *10*, 265.

Luk, K.C., Kehm, V., Carroll, J., Zhang, B., O'Brien, P., Trojanowski, J.Q., and Lee, V.M. (2012). Pathological alpha-synuclein transmission initiates Parkinson-like neurodegeneration in nontransgenic mice. Science *338*, 949-953.

Mariucci, G., Pagiotti, R., Galli, F., Romani, L., and Conte, C. (2018). The Potential Role of Toll-Like Receptor 4 in Mediating Dopaminergic Cell Loss and Alpha-Synuclein Expression in the Acute MPTP Mouse Model of Parkinson's Disease. J Mol Neurosci *64*, 611-618.

Marras, C., Beck, J.C., Bower, J.H., Roberts, E., Ritz, B., Ross, G.W., Abbott, R.D., Savica, R., Van Den Eeden, S.K., Willis, A.W.*, et al.* (2018). Prevalence of Parkinson's disease across North America. NPJ Parkinsons Dis *4*, 21.

Meredith, G.E., and Rademacher, D.J. (2011). MPTP mouse models of Parkinson's disease: an update. J Parkinsons Dis *1*, 19-33.

Meredith, G.E., Totterdell, S., Petroske, E., Santa Cruz, K., Callison, R.C., Jr., and Lau, Y.S. (2002). Lysosomal malfunction accompanies alpha-synuclein aggregation in a progressive mouse model of Parkinson's disease. Brain Res *956*, 156-165.

Meredith, G.E., Totterdell, S., Potashkin, J.A., and Surmeier, D.J. (2008). Modeling PD pathogenesis in mice: advantages of a chronic MPTP protocol. Parkinsonism Relat Disord *14 Suppl 2*, S112-115.

Michel, P.P., and Hefti, F. (1990). Toxicity of 6-hydroxydopamine and dopamine for dopaminergic neurons in culture. J Neurosci Res *26*, 428-435.

Moon, H.E., and Paek, S.H. (2015). Mitochondrial Dysfunction in Parkinson's Disease. Exp Neurobiol *24*, 103-116.

Mouradian, M.M. (2002). Recent advances in the genetics and pathogenesis of Parkinson disease. Neurology *58*, 179-185.

Muroyama, A., Kobayashi, S., and Mitsumoto, Y. (2011). Loss of striatal dopaminergic terminals during the early stage in response to MPTP injection in C57BL/6 mice. Neurosci Res *69*, 352-355.

Mytilineou, C., Walker, R.H., JnoBaptiste, R., and Olanow, C.W. (2003). Levodopa is toxic to dopamine neurons in an in vitro but not an in vivo model of oxidative stress. J Pharmacol Exp Ther *304*, 792-800.

Nakai, M., Fujita, M., Waragai, M., Sugama, S., Wei, J., Akatsu, H., Ohtaka-Maruyama, C., Okado, H., and Hashimoto, M. (2007). Expression of alpha-synuclein, a presynaptic protein implicated in Parkinson's disease, in erythropoietic lineage. Biochem Biophys Res Commun *358*, 104-110.

Naoi, M., and Maruyama, W. (1999). Cell death of dopamine neurons in aging and Parkinson's disease. Mech Ageing Dev *111*, 175-188.

Nath, S., Goodwin, J., Engelborghs, Y., and Pountney, D.L. (2011). Raised calcium promotes alpha-synuclein aggregate formation. Mol Cell Neurosci *46*, 516-526.

Nicholls, D.G. (2009). Mitochondrial calcium function and dysfunction in the central nervous system. Biochim Biophys Acta *1787*, 1416-1424.

Nicholls, D.G., and Budd, S.L. (1998). Neuronal excitotoxicity: the role of mitochondria. Biofactors *8*, 287-299.

Nussbaum, R.L., and Ellis, C.E. (2003). Alzheimer's disease and Parkinson's disease. N Engl J Med *348*, 1356-1364.

Oorschot, D.E. (1996). Total number of neurons in the neostriatal, pallidal, subthalamic, and substantia nigral nuclei of the rat basal ganglia: a stereological study using the cavalieri and optical disector methods. J Comp Neurol *366*, 580-599.

Ortner, N.J. (2021). Voltage-Gated Ca(2+) Channels in Dopaminergic Substantia Nigra Neurons: Therapeutic Targets for Neuroprotection in Parkinson's Disease? Front Synaptic Neurosci *13*, 636103.

Ortner, N.J., Bock, G., Dougalis, A., Kharitonova, M., Duda, J., Hess, S., Tuluc, P., Pomberger, T., Stefanova, N., Pitterl, F.*, et al.* (2017). Lower Affinity of Isradipine for L-Type Ca(2+) Channels during Substantia Nigra Dopamine Neuron-Like Activity: Implications for Neuroprotection in Parkinson's Disease. J Neurosci *37*, 6761-6777.

Pagano, G., Taylor, K.I., Anzures-Cabrera, J., Marchesi, M., Simuni, T., Marek, K., Postuma, R.B., Pavese, N., Stocchi, F., Azulay, J.P.*, et al.* (2022). Trial of Prasinezumab in Early-Stage Parkinson's Disease. N Engl J Med *387*, 421-432.

Parkinson, J. (2002). An essay on the shaking palsy. 1817. J Neuropsychiatry Clin Neurosci *14*, 223-236; discussion 222.

Parkinson Study, G. (2013). Phase II safety, tolerability, and dose selection study of isradipine as a potential disease-modifying intervention in early Parkinson's disease (STEADY-PD). Mov Disord *28*, 1823-1831.

Parkinson Study Group, S.-P.D.I.I.I.I. (2020). Isradipine Versus Placebo in Early Parkinson Disease: A Randomized Trial. Ann Intern Med *172*, 591-598.

Paxinos, G., and Franklin, K. (2001). The Mouse Brain in Stereotaxic Coordinates, 2 edn (San Diego: Academic Press).

Periquet, M., Fulga, T., Myllykangas, L., Schlossmacher, M.G., and Feany, M.B. (2007). Aggregated alpha-synuclein mediates dopaminergic neurotoxicity in vivo. J Neurosci *27*, 3338-3346.

Platzer, J., Engel, J., Schrott-Fischer, A., Stephan, K., Bova, S., Chen, H., Zheng, H., and Striessnig, J. (2000). Congenital deafness and sinoatrial node dysfunction in mice lacking class D L-type Ca2+ channels. Cell *102*, 89-97.

Poetschke, C., Dragicevic, E., Duda, J., Benkert, J., Dougalis, A., DeZio, R., Snutch, T.P., Striessnig, J., and Liss, B. (2015). Compensatory T-type Ca2+ channel activity alters D2-autoreceptor responses of Substantia nigra dopamine neurons from Cav1.3 L-type Ca2+ channel KO mice. Sci Rep *5*, 13688.

Poewe, W., Seppi, K., Tanner, C.M., Halliday, G.M., Brundin, P., Volkmann, J., Schrag, A.E., and Lang, A.E. (2017). Parkinson disease. Nat Rev Dis Primers *3*, 17013.

Polymeropoulos, M.H., Lavedan, C., Leroy, E., Ide, S.E., Dehejia, A., Dutra, A., Pike, B., Root, H., Rubenstein, J., Boyer, R.*, et al.* (1997). Mutation in the alpha-synuclein gene identified in families with Parkinson's disease. Science *276*, 2045-2047.

Przedborski, S., Jackson-Lewis, V., Naini, A.B., Jakowec, M., Petzinger, G., Miller, R., and Akram, M. (2001). The parkinsonian toxin 1-methyl-4-phenyl-1,2,3,6-tetrahydropyridine (MPTP): a technical review of its utility and safety. J Neurochem *76*, 1265-1274.

Purves, D., Augustine, G., Fitzpatrick, D., Hall, W., LaMantia, A., White, L., Mooney, R., and Platt, M. (2018). Neuroscience, 6 edn (Oxford University Press).

Quinn, P.M.J., Moreira, P.I., Ambrosio, A.F., and Alves, C.H. (2020). PINK1/PARKIN signalling in neurodegeneration and neuroinflammation. Acta Neuropathol Commun *8*, 189.

Rabey, J., and Burns, R. (2002). In: Dopamine Metabolites, in Parkinson's Disease: Diagnosis and Clinical Management, 2 edn (New York: Demos Medical Publishing).

Raff, M.C., Whitmore, A.V., and Finn, J.T. (2002). Axonal self-destruction and neurodegeneration. Science *296*, 868-871.

Rcom-H'cheo-Gauthier, A.N., Meedeniya, A.C., and Pountney, D.L. (2017). Calcipotriol inhibits alpha-synuclein aggregation in SH-SY5Y neuroblastoma cells by a Calbindin-D28k-dependent mechanism. J Neurochem *141*, 263-274.

Recasens, A., Dehay, B., Bove, J., Carballo-Carbajal, I., Dovero, S., Perez-Villalba, A., Fernagut, P.O., Blesa, J., Parent, A., Perier, C.*, et al.* (2014). Lewy body extracts from Parkinson disease brains trigger alpha-synuclein pathology and neurodegeneration in mice and monkeys. Ann Neurol *75*, 351-362.

Richardson, J.R., Quan, Y., Sherer, T.B., Greenamyre, J.T., and Miller, G.W. (2005). Paraquat neurotoxicity is distinct from that of MPTP and rotenone. Toxicol Sci *88*, 193-201.

Riederer, P., Konradi, C., Schay, V., Kienzl, E., Birkmayer, G., Danielczyk, W., Sofic, E., and Youdim, M.B. (1987). Localization of MAO-A and MAO-B in human brain: a step in understanding the therapeutic action of L-deprenyl. Adv Neurol *45*, 111-118.

Ritz, B., Rhodes, S.L., Qian, L., Schernhammer, E., Olsen, J.H., and Friis, S. (2010). L-type calcium channel blockers and Parkinson disease in Denmark. Ann Neurol *67*, 600-606.

Rocha Cabrero, F., and Morrison, E.H. (2022). Lewy Bodies. In StatPearls (Treasure Island (FL)).

Sagala, F.S., Harnack, D., Bobrov, E., Sohr, R., Gertler, C., James Surmeier, D., and Kupsch, A. (2012). Neurochemical characterization of the striatum and the nucleus accumbens in L-type Ca(v)1.3 channels knockout mice. Neurochem Int *60*, 229-232.

Salamon, A., Zadori, D., Szpisjak, L., Klivenyi, P., and Vecsei, L. (2020). Neuroprotection in Parkinson's disease: facts and hopes. J Neural Transm (Vienna) *127*, 821-829.

Schapira, A.H. (2008). Mitochondria in the aetiology and pathogenesis of Parkinson's disease. Lancet Neurol *7*, 97-109.

Schapira, A.H., Cooper, J.M., Dexter, D., Clark, J.B., Jenner, P., and Marsden, C.D. (1990). Mitochondrial complex I deficiency in Parkinson's disease. J Neurochem *54*, 823-827.

Schmidt, N., and Ferger, B. (2001). Neurochemical findings in the MPTP model of Parkinson's disease. J Neural Transm *108*, 1263-1282.

Sharon, R., Bar-Joseph, I., Frosch, M.P., Walsh, D.M., Hamilton, J.A., and Selkoe, D.J. (2003). The formation of highly soluble oligomers of alpha-synuclein is regulated by fatty acids and enhanced in Parkinson's disease. Neuron *37*, 583-595.

Singh, A., Mewes, K., Gross, R.E., DeLong, M.R., Obeso, J.A., and Papa, S.M. (2016). Human striatal recordings reveal abnormal discharge of projection neurons in Parkinson's disease. Proc Natl Acad Sci U S A *113*, 9629-9634.

Starkov, A.A. (2008). The role of mitochondria in reactive oxygen species metabolism and signaling. Ann N Y Acad Sci *1147*, 37-52.

Sulzer, D. (2007). Multiple hit hypotheses for dopamine neuron loss in Parkinson's disease. Trends Neurosci *30*, 244-250.

Sulzer, D., and Surmeier, D.J. (2013). Neuronal vulnerability, pathogenesis, and Parkinson's disease. Mov Disord *28*, 41-50.

Surmeier, D.J. (2018). Determinants of dopaminergic neuron loss in Parkinson's disease. FEBS J *285*, 3657-3668.

Surmeier, D.J., Guzman, J.N., and Sanchez-Padilla, J. (2010a). Calcium, cellular aging, and selective neuronal vulnerability in Parkinson's disease. Cell Calcium *47*, 175-182.

Surmeier, D.J., Guzman, J.N., Sanchez-Padilla, J., and Goldberg, J.A. (2010b). What causes the death of dopaminergic neurons in Parkinson's disease? Prog Brain Res *183*, 59-77.

Surmeier, D.J., Obeso, J.A., and Halliday, G.M. (2017a). Selective neuronal vulnerability in Parkinson disease. Nat Rev Neurosci *18*, 101-113.

Surmeier, D.J., Schumacker, P.T., Guzman, J.D., Ilijic, E., Yang, B., and Zampese, E. (2017b). Calcium and Parkinson's disease. Biochem Biophys Res Commun *483*, 1013-1019.

Tanner, C.M., Ross, G.W., Jewell, S.A., Hauser, R.A., Jankovic, J., Factor, S.A., Bressman, S., Deligtisch, A., Marras, C., Lyons, K.E*., et al.* (2009). Occupation and risk of parkinsonism: a multicenter case-control study. Arch Neurol *66*, 1106-1113.

Tansey, M.G., and Goldberg, M.S. (2010). Neuroinflammation in Parkinson's disease: its role in neuronal death and implications for therapeutic intervention. Neurobiol Dis *37*, 510-518.

Tatton, N.A., and Kish, S.J. (1997). In situ detection of apoptotic nuclei in the substantia nigra compacta of 1-methyl-4-phenyl-1,2,3,6-tetrahydropyridine-treated mice using terminal deoxynucleotidyl transferase labelling and acridine orange staining. Neuroscience *77*, 1037-1048.

Trinh, J., and Farrer, M. (2013). Advances in the genetics of Parkinson disease. Nat Rev Neurol *9*, 445-454.

Ulusoy, A., Bjorklund, T., Buck, K., and Kirik, D. (2012). Dysregulated dopamine storage increases the vulnerability to alpha-synuclein in nigral neurons. Neurobiol Dis *47*, 367-377.

Uttara, B., Singh, A.V., Zamboni, P., and Mahajan, R.T. (2009). Oxidative stress and neurodegenerative diseases: a review of upstream and downstream antioxidant therapeutic options. Curr Neuropharmacol *7*, 65-74.

Venda, L.L., Cragg, S.J., Buchman, V.L., and Wade-Martins, R. (2010). alpha-Synuclein and dopamine at the crossroads of Parkinson's disease. Trends Neurosci *33*, 559-568.

Vila, M., Ramonet, D., and Perier, C. (2008). Mitochondrial alterations in Parkinson's disease: new clues. J Neurochem *107*, 317-328.

Vila, M., Vukosavic, S., Jackson-Lewis, V., Neystat, M., Jakowec, M., and Przedborski, S. (2000). Alpha-synuclein up-regulation in substantia nigra dopaminergic neurons following administration of the parkinsonian toxin MPTP. J Neurochem *74*, 721-729.

Wang, Q.M., Xu, Y.Y., Liu, S., and Ma, Z.G. (2017). Isradipine attenuates MPTP-induced dopamine neuron degeneration by inhibiting up-regulation of L-type calcium channels and iron accumulation in the substantia nigra of mice. Oncotarget *8*, 47284-47295.

Winklhofer, K.F., and Haass, C. (2010). Mitochondrial dysfunction in Parkinson's disease. Biochim Biophys Acta *1802*, 29-44.

Xu, Z., Cawthon, D., McCastlain, K.A., Slikker, W., Jr., and Ali, S.F. (2005). Selective alterations of gene expression in mice induced by MPTP. Synapse *55*, 45-51.

Zampese, E., and Surmeier, D.J. (2020). Calcium, Bioenergetics, and Parkinson's Disease. Cells *9*.

Zamponi, G.W., Striessnig, J., Koschak, A., and Dolphin, A.C. (2015). The Physiology, Pathology, and Pharmacology of Voltage-Gated Calcium Channels and Their Future Therapeutic Potential. Pharmacol Rev *67*, 821-870.

Zecca, L., Zucca, F.A., Wilms, H., and Sulzer, D. (2003). Neuromelanin of the substantia nigra: a neuronal black hole with protective and toxic characteristics. Trends Neurosci *26*, 578-580.

Zhu, J., and Chu, C.T. (2010). Mitochondrial dysfunction in Parkinson's disease. J Alzheimers Dis *20 Suppl 2*, S325-334.

8 Statutory Declaration

"I, Qingzhou Fei, by personally signing this document in lieu of an oath, hereby affirm that I prepared the submitted dissertation on the topic 'Modulatory effects of Cav1.3 calcium channels on dopamine homeostasis and alpha synuclein expression in a mouse model of Parkinson's disease'; (Der deutsche Titel: 'Die modulatorische Rolle von Calciumkanälen vom Subtyp Cav1.3 auf die Dopaminhomöostase und die Alpha-Synuclein-Expression in einem Mausmodell für den Morbus Parkinson')'', independently and without the support of third parties, and that I used no other sources and aids than those stated.

All parts which are based on the publications or presentations of other authors, either in letter or in spirit, are specified as such in accordance with the citing guidelines. The sections on methodology (in particular regarding practical work, laboratory regulations, statistical processing) and results (in particular regarding figures, charts and tables) are exclusively my responsibility.

Furthermore, I declare that I have correctly marked all of the data, the analyses, and the conclusions generated from data obtained in collaboration with other persons, and that I have correctly marked my own contribution and the contributions of other persons (cf. declaration of contribution). I have correctly marked all texts or parts of texts that were generated in collaboration with other persons.

My contributions to any publications to this dissertation correspond to those stated in the below joint declaration made together with the supervisor. All publications created within the scope of the dissertation comply with the guidelines of the ICMJE (International Committee of Medical Journal Editors; www.icmje.org) on authorship. In addition, I declare that I shall comply with the regulations of Charité – Universitätsmedizin Berlin on ensuring good scientific practice.

I declare that I have not yet submitted this dissertation in identical or similar form to another Faculty.

The significance of this statutory declaration and the consequences of a false statutory declaration under criminal law (Sections 156, 161 of the German Criminal Code) are known to me."

Date Signature

9 Curriculum Vitae

My curriculum vitae does not appear in the electronic version of my paper for reasons of data protection.

10 Acknowledgements

First, I would like to thank Prof. Andrea Kühn for providing me with the opportunity starting a doctoral study at Charite. I would like to acknowledge Prof. Franz Theuring providing lab facility and continuous support for my study and experiment. I am grateful to Dr. Daniel Harnack for providing me with the interesting topic and supervising my doctoral thesis. Many thanks to Dr. Karima Schwab for teaching me experimental skills patiently and huge support for my thesis. Also, many thanks to Ferry Sagala for his help and support at the beginning of my study.

I am most grateful to my family. I deeply thank my parents for their love and confidence in me. I owe many thanks to my wife Dr. Tian Zhang who took care of me with love, provided invaluable advice and encouraged me through all difficulties. Finally, I would like to express my gratitude to my two little children Grace and Noah. Their smile always makes me feel relieved.